Georgia Tech Sponsored Research

Project   E-16-N20

Project director   Mavris   Dimitri

Research unit   Aero Engr

Title   Advanced Design Methodology for Robust Aircraft
                       Sizing and Synthesis

Project date   7/31/1999

NAG-1-1793

Advanced Design Methodology for

Robust Aircraft Sizing and Synthesis

Year 1 Progress Report

November 1996

Dimitri N. Mavris
Principal Investigator

Aerospace Systems Design Laboratory
School of Aerospace Engineering
Atlanta, GA 30332-0150

Summary

The goal of designing for robustness is achieved by minimizing a configuration's sensitivity to the uncertainty factors, which themselves may take various forms (economic, mission related, disciplinary). The result is a solution which satisfies the customer requirements while at the same time is well-balanced in that it performs well under a wide variation of conditions. This report documents a method by which robust aircraft designs are obtained, utilizing a new probabilistic objective function and making use of techniques such as Response Surface Method and Monte Carlo simulation. Three detailed implementation examples of the robust design simulation (RDS) are presented addressing various forms of design uncertainty. Additionally, in accordance with Year one objectives, an initial investigation into the merits of Neural Networks and Fuzzy Logic was completed to determine their potential merits in the RDS environment. Prospects and directions for Year two research are outlined to complete the report.

Acknowledgments

Table of Contents

List of Illustrations

List of Tables

1. Introduction

In a *traditional* aircraft design problem, an engineer seeks to find the settings of a preselected group of design variables which minimize a specified objective function. The concept of *robust* aircraft design, however, entails a further decomposition of terms. The group of available design variables must be classified into two distinct categories: those that the designer may freely vary and those which may vary, but are outside of the control of the designer. The first group termed are control variables while the second group represents noise (or uncertainty) variables.

The goal of designing for robustness is achieved by minimizing a configuration's sensitivity to the uncertainty factors, which themselves may take various forms (economic, mission related, disciplinary). This is accomplished not by optimizing a single quantity, but rather by simultaneously minimizing variation associated with the selected quantity as well finding its optimum value (or meeting its target). The result is a solution which satisfies the customer requirements while at the same time is well-balanced in that it performs well under a wide variation of conditions.

Since any system analysis or optimization is only as good as the quality of the contributing analyses, the need for introducing higher fidelity, discipline-specific analyses in the methodology is apparent. This need provides the impetus for the use of Response Surface Equations (RSEs). RSEs allow one to enhance or improve the synthesis program's analyses capabilities and make possible the study of innovative aircraft concepts and technologies using more sophisticated method. A key requirement is that these RSEs must accurately represent the data generated by the sophisticated codes. Recognizing that this accuracy may not always be possible through RSEs, a portion of this study is dedicated to seeking improved techniques for the enhancement of ASDL's robust design simulation (RDS). In Year one, this emphasis has resulted in the investigation of

RSE transformations as well as new approximation techniques to ensure that, when obstacles do arise in executing the RDS, alternate avenues will be available to overcome them.

After a short review of the Year one tasks for this study, sections II-IV will describe Year one research results and conclusions. The report closes with an overall summary and ideas for future directions. Publications which have resulted from this research and some related references are listed after the summary.

1.1. Year One Tasks

* Develop a procedure according to which a Robust Design Simulation can be achieved
* Classify forms of uncertainty (design, environmental, etc.)
* Identify the dependencies between noise variables and the OEC for a range of control variable settings
* Develop disciplinary (aerodynamics, structures, etc.) RSEs for differing classes of vehicles using such codes as ELAPS, BDAP, AWAVE, etc.
* Initiate information gathering/literature search on Neutral Networking, Genetic Algorithm, Fuzzy Logic

1.2. Classroom Case Study

It is a continual goal at ASDL to incorporate research results directly into the classroom environment through lectures and focused projects. The evolving RDS method described below and the associated examples of addressing various forms of uncertainty were presented to students in the core classes of the School of AE's design curriculum (AE 6351 and AE 6352) in the winter and spring terms of 1996. These students subsequently implemented the RDS for an HSCT, with specific emphasis on designing and forming disciplinary RSEs in a number of areas. A full length report documenting the students effort is in the final stages of preparation and will be made

available once completed under separate cover. Below are some details which summarize their objectives, analyses, and results.

Every year, ASDL sponsors a graduate design team as part of the aerospace graduate curriculum. The purpose of the design team is to create a conceptual/preliminary aircraft design by applying the methods learned in class to the design and synthesis of an aerospace vehicle of current interest. The motivating idea is to teach students practical implementation of advanced design methodologies via a focused design project. This year's project was the Robust Design of a High Speed Civil Transport (HSCT).

The thrust of the 1996 team's work was to extend the methods pioneered by the previous year's design team and apply RDS methods developed in ASDL research over the past year. This was accomplished by focusing on several primary objectives:

- Design a feasible, economically viable HSCT

  Bring various disciplines together via Integrated Product Teams (IPT) to demonstrate the utility of RDS and IPPD in the aircraft design process; utilize RSM where appropriate to accomplish this

- Develop "design skills" and foster a spirit of teamwork among team members

In pursuing these objectives, the central accomplishment of this year's design team was the application of response surface methods (RSM) in several disciplines concurrently to create a truly conceptual/preliminary IPPD tool (based on FLOPS). These disciplinary RSEs included ones involving structures, aircraft noise, and static stability. Once the new FLOPS tool was created, two parallel approaches to robust design were carried out, one based on ASDL's RDS and the other based on an approach developed in Georgia Tech's School of Mechanical Engineering. The results of the two implementations provided some interesting similarities (and a few differences).

The report currently being prepared details the methods, results, and lessons learned during the 1996 HSCT design project. The intent is to provide a roadmap of what has been accomplished to date in the area of robust design of HSCT configurations so that future teams can extend the methods used here. The information contained in it should be sufficient for a relative newcomer to

the field of robust design to understand the methods used and apply them to other areas of design such as rotorcraft, space vehicles, etc.

2. Objective Functions in a Robust Design Simulation

2.1. Forming an Initial Overall Evaluation Criterion

As mentioned in the introduction, the goal of designing for robustness is achieved by minimizing a configuration's sensitivity to a variety of design uncertainties. This is not accomplished by solely optimizing the mean of an objective function, but rather by minimizing variation, or variance, associated with the selected objective as well. Taguchi introduced the concept of a signal-to-noise-ratio (S/N) which, if maximized, yields a high signal or benefit with little noise or variation[6],[7],[8]. This solution satisfies the customer requirements while at the same time is well-balanced in that it performs well under a wide variation of conditions and environments. In an effort to improve on Taguchi's signal-to-noise-ratio concept, ASDL introduced and examined a new metric, based more on statistical foundations. In this new approach, traditional design objectives such as weight, life cycle cost, or ticket price now become intermediate evaluation metrics used to construct a new objective, the Overall Evaluation Criterion (OEC), which will ultimately be minimized.

This OEC is comprised of the mean and variance of the traditional design objective, and they are computed based on the presence of uncertainty variables in the design space. The three equations listed below are the mathematical formulations of the desired OEC for three different design objectives: minimizing the objective, maximizing it, and optimizing it for a specified target value. Equation (1), the product of variance and the square of the mean, is analogous to the traditional concept of single objective minimization. Equation (2) is in turn analogous to single objective maximization. Finally, Equation (3), a weighted average of the variance and the squared deviation from the target, represents the case where the objective is to minimize the deviation from a specified target value. A summation has been employed here rather than a product, since a value for the mean right on the target would yield an OEC of zero using the product regardless of the

associated variance. In this case, α is an arbitrarily chosen weighting parameter that can emphasize either distance from target value or variation. *However, for all three equations, a minimal value for the OEC is desired.*

$$OEC = Variance * Mean^2 \quad \text{(minimize mean for traditional objective)} \quad (1)$$

$$OEC = Variance / Mean^2 \quad \text{(maximize mean for traditional objective)} \quad (2)$$

$$OEC = \alpha * (Mean - Target)^2 + (1-\alpha) * Variance \quad (3)$$

Minimizing one of these of OECs is equivalent to maximizing the signal-to-noise ratio according to Taguchi's formulation. The two methods differ, however, in the way this OEC or signal-to-noise ratio is obtained. While Taguchi's approach utilizes an inner and outer array for design and noise variables respectively[6],[7], the RDS OEC is based on a Design of Experiment (DOE) implementation which yields RSEs as a function of all key design and noise variables. In this case, the noise variables are assigned probability shape functions that produce, through a Monte Carlo simulation, a probability distribution for the objective, $/RPM. This approach to the estimation of the noise factor effects represents a major improvement in accuracy compared to Taguchi's approach.

2.2. Extensions to the OEC Concept

As experimentation with the use of the OECs in Eq. (1-3) proceeded, new ideas came to light. The following steps describe an extension developed to these OEC formulations. A DOE table, independent of any that were used in previous steps of RDS up to that point, is constructed for the control variables only. For each case in this DOE (i.e. for each setting of the control variables), a Monte Carlo simulation is being executed based on the assumptions made for the

noise variables, which are in general non-normal distributions. Note that this process encompasses numerous simulations, each of which requires 5,000-10,000 function calls! Without the facilitation of RSEs, this is an almost impossible task to accomplish. In addition, the Monte Carlo simulation has been chosen over an available analytical method for the distribution generation, since Monte Carlo does not need the simplifying assumption of normal distributions for the noise variables. Each of the simulations defined in the DOE generates a frequency chart for the objective, similar to the one in Figure 1.
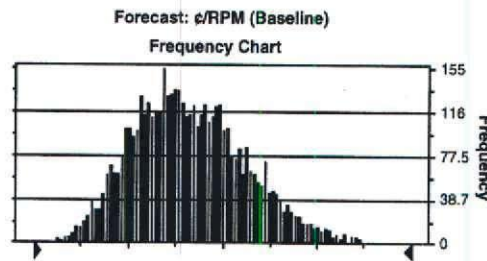
Figure 1. Example Distribution for the Objective

Figure 1 is a frequency chart. What is desired, however, is an analytical expression for the probability distribution represented by the frequency chart. In order to achieve this, each frequency distribution is approximated by one of the standard probability distributions. This distribution fitting process, employed by Crystal Ball® [Ref. 1], has been found to most often yield a gamma distribution, displayed in Equation 4, as the best approximation via the Chi-Square Ranking Method. By keeping track of the location (L), scale (α), and shape (β) for each distribution of each run in the DOE table, a response surface equation in terms of the control variables in the table can be fitted for each of the 3 parameters.

$$f(x) = \frac{(\frac{x-L}{\alpha})^{\beta-1} \cdot e^{-(\frac{x-L}{\alpha})}}{\alpha \cdot \Gamma(\beta)} \qquad (4)$$

However, attempting to do this has shown that the fit of a quadratic equation for the gamma distribution parameters is generally very poor (R-square between 40 and 80%). Hence, a new direction was again postulated.

The latest proposed methodology employs the fit of an RSE for the probability of achieving objective function values below a desired target value P(Obj≤target) that can generally be fit much better to the obtained data (R-square of 92 to 98%). In other words, the obtained equation links a customers objective of achieving values smaller than a target to design or control variables that allow the designer to optimize the objective in order to find the design solution that guaranties the probability of customer satisfaction. After having obtained this equation in terms of the central variables, an optimal solution can easily be found by maximizing P(Obj≤target) while satisfying all imposed design and environmental constraints. This optimal solution corresponds to a shift of the objective distribution for the objective as displayed in Figure 2. The ability to perform a constrained optimization is one of the advantages of this method over, for example, the Taguchi method. [Ref. 2]
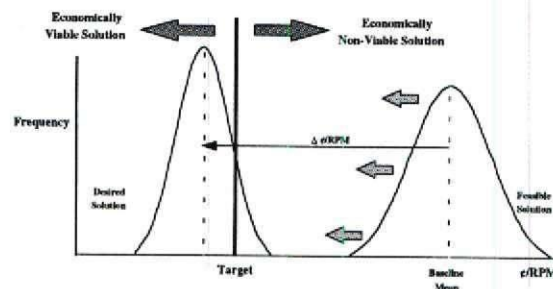
Figure 2. Distribution Shift to Maximize Probability of Achieving a Target

3. Uncertainty and the use of RSEs in Robust Design Simulation

3.1. *Economic Uncertainty with System Level RSEs*

Economic uncertainty, not considered in traditional aircraft design environments, has been found over the past two years at ASDL to significantly affect the economic viability of a fleet of vehicles, often more significant than technology considerations. Although there are a wide variety of economic uncertainties, key quantities that have been used in recent RDS problems include fuel cost, economic range, and load factor. Uncertainty in fuel cost is fairly obvious, since surely its price will fluctuate over the life of an aircraft. The economic range represents the average mission distance the aircraft will fly over its life, a quantity needed for the estimation of direct operating cost. For example an HSCT will service cities that are at least 3,000nm apart and most likely on the average 3,200nm apart even though aircraft is sized for around 5,000nm. Load Factor is strictly an economical factor, describing the ratio of passengers boarded on a given trip to available seats. Its mode is assumed to be at 65%. Economic analysis is done using the Aircraft Life Cycle Cost Analysis (ALCCA) program, which takes, among other inputs, the component weights and fuel weight from a converged FLOPS sizing run. ALCCA also accounts for airline and manufacturer business practices (e.g. required return on investments). [Ref. 3]

The following example from Reference 4 demonstrates the modeling of economic uncertainty. The task is to find a robust design for a HSCT, emphasizing wing planform and engine cycle control parameters. Additionally, takeoff and landing field length limitations (less than 11,000ft) are imposed. The design objective, ¢/RPM, and all constraints considered for this example are summarized in Table 1.

Table 1. Summary of Objective and Constraints for Economic Uncertainty Example

Response	Requirement
¢/RPM	minimize
Acquisition Cost	minimize
Gross Weight	N/A
Fuel Requirement Rf	> 1
Approach Speed	< 154 kts
Takeoff Field Length	< 10,500 ft
Landing Field Length	< 11,000 ft

All responses presented in Table 1 are modeled by FLOPS/ALCCA as functions of design/control and noise variables. In order to facilitate the Monte Carlo simulation without executing the actual synthesis code for each simulation run, each of the responses is approximated by an RSE in terms of the most important design/control and noise variables, according to the Pareto Principle.

For this example, the six most important control factors, presented in Table 2, were selected together with the three most influential economic noise quantities. These noise variables presented in Table 2 as well and are responsible for the fact that the final objective well be a probability distribution for the ¢/RPM. The economic noise variables influence economic responses only, hence introducing a distribution to ¢/RPM and acquisition cost only.

Table 2. Summary of Control and Noise Variables

Variable	Type	Name	Range
Thrust to Weight Ratio	Control	TWR	0.28 - 0.32
Wing Area	Control	WingArea	8.5 - 9.5 10^3 ft^2
Longitudinal Kink Location	Control	x1	1.54 - 1.62
Spanwise Kink Location	Control	y1	0.5 - 0.58
Turbine Inlet Temperature	Control	TIT	3 - 3.25 10^3 °F
Fan Pressure Ratio	Control	FPR	3.5 - 4.5
Fuel Cost	Noise	$-Fuel	0.55 - 1.1 $/gal
Load Factor	Noise	LF	0.55 - 0.75
Economic Range	Noise	Ec-Range	3 - 5 10^3 nm

The ranges for all variables which describe the design space are shown in Table 2. Thrust to Weight Ratio is one of the main sizing variables describing the ratio of engine thrust over the gross weight of the vehicle. Wing area replaces wing loading as a sizing variable and contributes also as an aerodynamic variable. The kink location, normalized by the semispan, was found in a previous ASDL study to be the main aerodynamic effect contributing to the objective, ¢/RPM, and the constraints. [Ref. 5]

Turbine Inlet Temperature and Fan Pressure Ratio are the main propulsion related variables contributing to the objective function and the constraints. Fuel Cost is modeled over the life of the aircraft and includes the rather unlikely cases of oil crises, yielding the relatively large variation. However, the mode of its distribution is assumed to be at 0.65$/gal. The previously mentioned Load Factor has a mode of 65%. It is assumed also that the HSCT will service cities that are at least 3,000nm and most likely on the average 3,200nm apart. Nevertheless, the current configuration is capable of flying distances below 5,000nm, the upper limit for this variable.

The equations for probability of achieving objective values (¢/RPM, seen as Y in Figure 3) below the target values A, B, C, and D together with the ¢/RPM, acquisition cost, gross weight, and the constraints are displayed in Figure 3 in the form of prediction profiles. Also shown is the robust design solution based on its so called desirability, a feature of JMP® [Ref. 6], the statistical package used to generate the DOEs, equations, and all prediction profile graphs presented in this

report. JMP® assigns desirability values between zero and one (bottom row of Figure 3), one being the most desirable, to all design variable settings based on assigned desirability values for each response. For example, if a response is supposed to be maximized, like Prob(Y≤A), high values of that response are assigned high desirability values, as displayed in the last column of Figure 3. If a response is supposed to be minimized, like the objective function ¢/RPM, high desirability values are assigned to low values for that response. By perturbing the variable setting, each outcome of a response yields a desirability for that setting based on the assigned desirability. If more desirabilities are being assigned to different responses, all desirabilities are multiplied with each other. This allows a multiple objectives optimization that is translated into a single objective, called desirability.
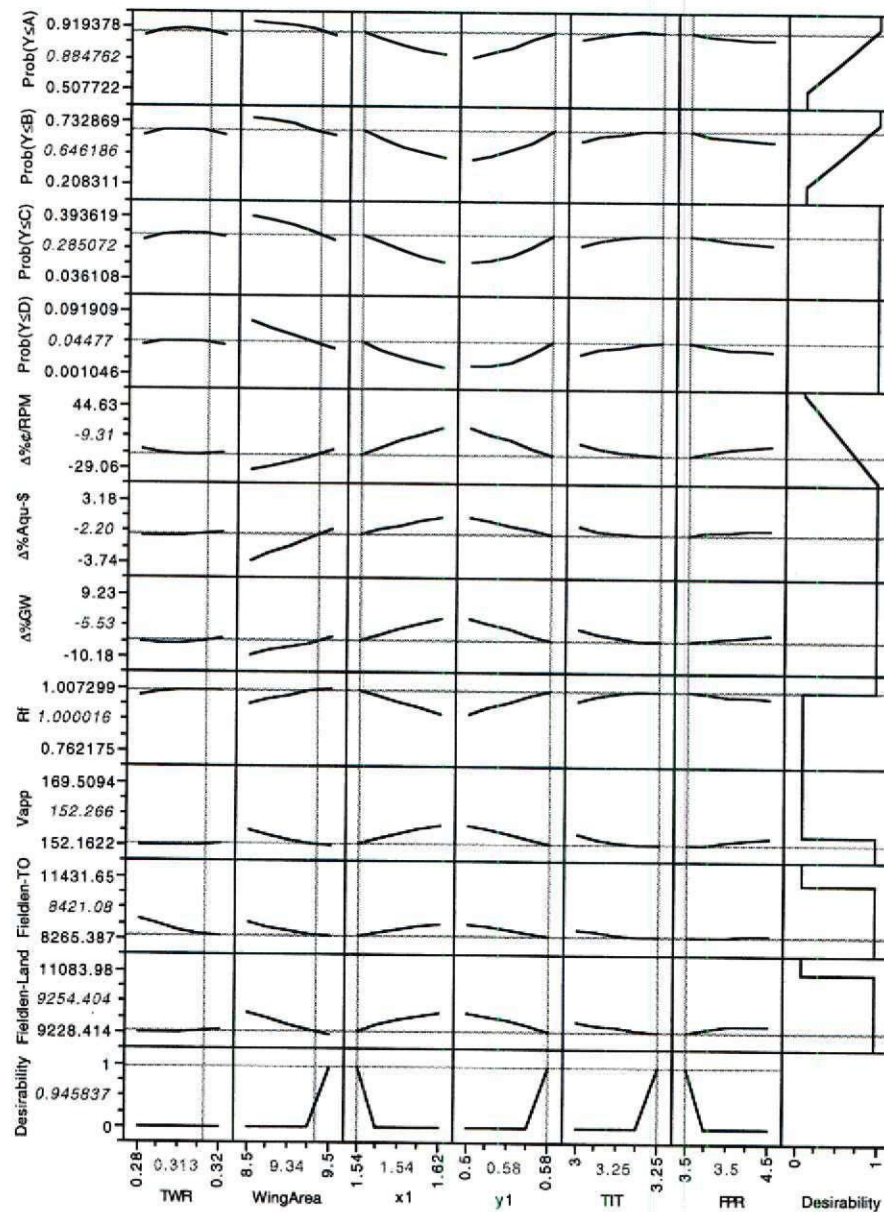
Figure 3. Prediction Profiles for Probabilities, Objectives, and Constraints

Additionally, this desirability feature is able to handle constraints by assigning a desirability of zero to all constraint response values that violate their requirement and one to those that satisfy the value. Hence, all variable settings that violate a constraint will have a desirability of zero since the desirabilities of all responses are multiplied. If a response, such as gross weight, should not influence the desirability value of the solution, all values are being assigned a desirability of one. This feature enables the designer to obtain a solution to an optimization problem quickly and very

visibly on the screen without the need for a separate optimization execution. The obtained robust design solution as it compares with the baseline are summarized in Table 3.

Table 3. RDS Solution for Economic Uncertainty Example

Parameter	Robust Solution	Baseline
T/W Ratio	0.313	0.300
Wing Area	9340 ft²	9000 ft²
x1	1.54 x span	1.58 x span
y1	0.58 x span	0.54 x span
TIT	3250°F	3125°F
FPR	3.5	4.0

Based on the results presented in Table 3, a Monte Carlo simulation was employed one more time in order to compare the cumulative distribution for ¢/RPM of this robust design solution to the original one of the baseline, as displayed in Figure 4. For all targets, the robust design solution yields a higher probability of achieving values below that target. Naturally the probability increases with increasing values for the target. However, it can be seen that for "small" and "very large" target values the difference in probability between the robust design solution and the baseline is very small. The difference increases, however, for values around the means of the distributions. Hence, one can also conclude from this example that the improvement of one solution over another does depend on the target itself. Finally the entire exercise demonstrates a repeatable methodology for assessing economic uncertainty.
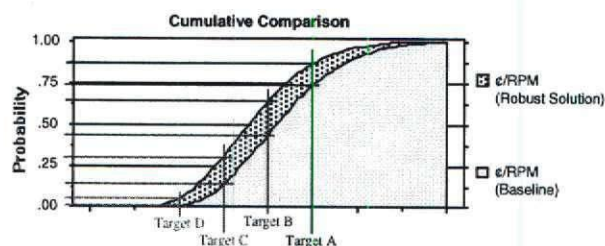
Figure 4. Distribution Comparison Between Baseline and Robust Design Solution

3.2. Mission Uncertainty with System Level RSEs

Since a transport aircraft flies a variety of different missions during its lifetime, the notion of sizing the aircraft for a "design mission" appears inadequate. It is proposed here that the eventual mix of city pairs that will make up the routes for an aircraft such as the HSCT is best represented by modeling the mission variability directly. Each city pair represents a distinct mission, with numerous possible active constraints, not the least of which is the requirement of subsonic flight over land. The length of the design mission is taken as a control variable. In other words, it can be chosen to achieve some optimum for a selected objective. The characteristics of the mission, however, are treated randomly, as illustrated in Figure 5. Due to the FAA stipulation of no supersonic flight over land, an HSCT must fly in regimes (subsonic and supersonic cruise) which cause conflicts in the planform optimization process. Thus, these optimizations generally result in geometry trades between subsonic and supersonic performance. Depending on the city pairs, the percentage of the mission flown at subsonic speeds will be different, thus affecting these trades. The most demanding mission is mission (a) in Figure 5 with a range of 6000 nm.
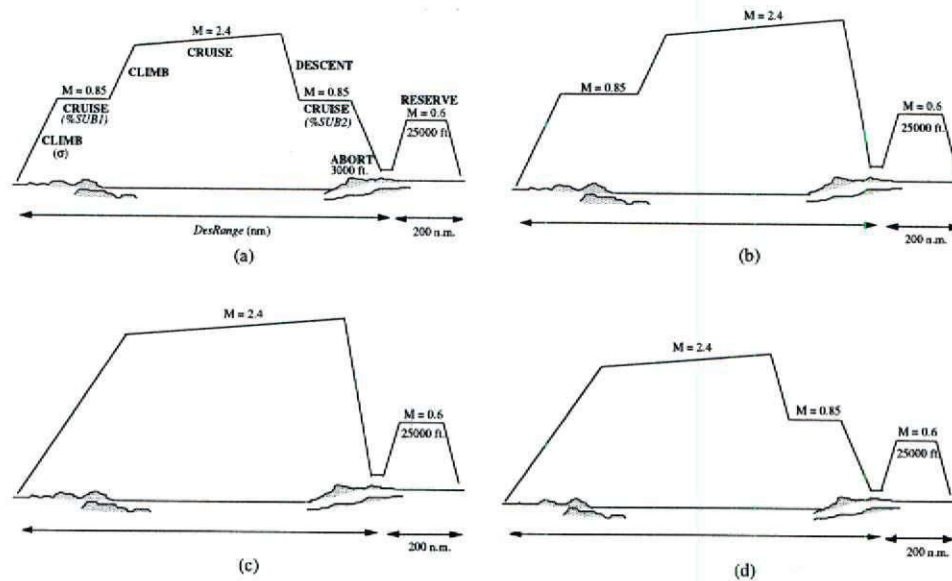
Figure 5. Possible HSCT Mission Profiles

To examine the effects of this mission uncertainty, intermediate RSEs similar to the economic uncertainty example above were formed which relate outputs such as the $/RPM to the control and noise variables. In this case, the control variables were mainly wing planform parameters while the noise variables consisted of a combination of mission and economic uncertainty terms. The RSEs themselves are best viewed via prediction profiles as seen in Figure 6. These RSEs relate the 10 variables to the five responses ($/RPM, Gross Weight, Fuel Weight, Takeoff Field Length, and Approach Speed). These responses can be thought of as intermediate objectives and constraints, since the ultimate objective and constraints will be *probabilities of achieving certain targets* for these intermediate responses. In the figure, the values of "-1" and "1" are normalizations of the respective actual minimum and maximum values, used to provide proper scaling between the 10 design variables. Table 4 shows the design variable and their range.

Table 4: HSCT Problem Design Variables and Classifications

Type	Variable	Group	Symbol	Minimum	Maximum
Control	Wing Kink X-location	Aerodynamic	X1	1.54	1.69
	Wing Kink Y-location	Aerodynamic	Y1	0.44	0.58
	Wing Ref. Area	Sizing	Sref	8500 sq. ft.	9500 sq. ft.
	Thrust/Weight	Sizing	TWR	0.28	0.32
	Mission Range	Mission	DESRNG	5000 nm	6000 nm
Random	%Subsonic- Leg1	Mission	SUBL1	0 %	15 %
	%Subsonic- Leg2	Mission	SUBL2	0 %	15 %
	Climb Optimization	Mission	CLIMB	0 (min time)	1 (min fuel)
	Fuel Cost	Economic	COFL	0.55 $/gal	1.1 $/gal
	Economic Range	Economic	EcRNG	3000 nm	5000 nm
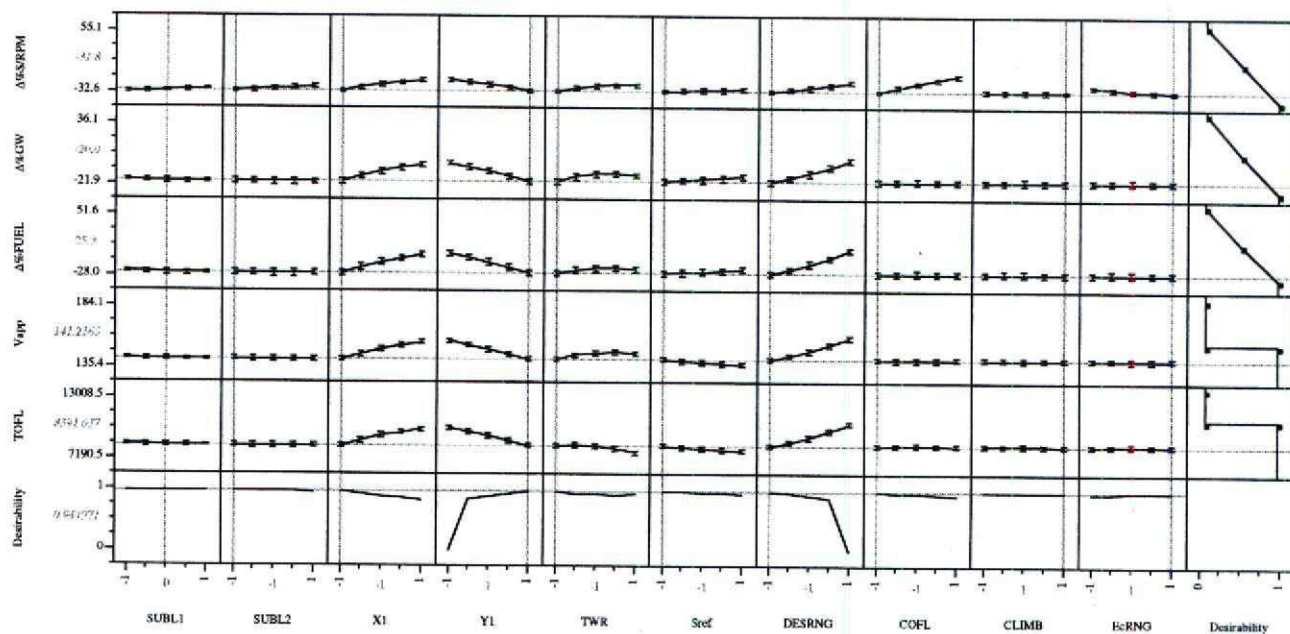
Figure 6. Prediction Profiles for Intermediate Objectives and Selected Constraints

Due to the noise variables, resulting robust design objective solutions will be in the form of probability distributions. In this particular case, the *constraints* as well as the objectives are affected by the uncertainty. Thus, they too will result in probability distributions. This phenomenon is due to the fact that the mission uncertainty affects the performance of the aircraft (unlike economic uncertainty, which does not). Now, to find a robust solution, the settings of

control variables which maximize the probability of meeting a target value for $/RPM while *simultaneously* achieving a probability of one (or very close to one) of meeting the constraints need to be determined. The desirability search procedure is utilized again by assigning a desirability of one to high probabilities of meeting three different targets for $/RPM. This is seen in Figure 6, showing the prediction profiles. Each response depicted represents a regression equation which relates the control parameters to a probability distribution for a given target. This is constrained by meeting the approach speed constraint for any possible combination of uncertainties. Thus, a probability of one of achieving a 154 knot approach speed is desired. Economic results are again normalized by the baseline.

As in the previous examples, targets are assigned for the $/RPM three targets are specified in Figure 7. Target A is the most aggressive since it represents the lowest $/RPM value of the three, followed in ascending order by B and C. Naturally, the probability of achieving the target increases from target A to C. Comparing against the intermediate (or traditional) desirability results of Figure 6, the robust search results show similar trends for three of the five control variables (*X1*, *TWR*, and *DESRNG*). The normalized y-kink location (*Y1*) takes on an intermediate value in the robust approach, and the wing area variable (*SREF*) should be set at its midpoint for the most robust feasible solution. The latter effect seems to be due to the conflicting goals of maximizing the probability of meeting the approach speed constraint and maximizing the achievement of low $/RPM targets. The other performance constraints tracked, the takeoff and landing field lengths, both resulted in probabilities of one for *every* point tested in the region of good designs. In other words, these constraints are not active.
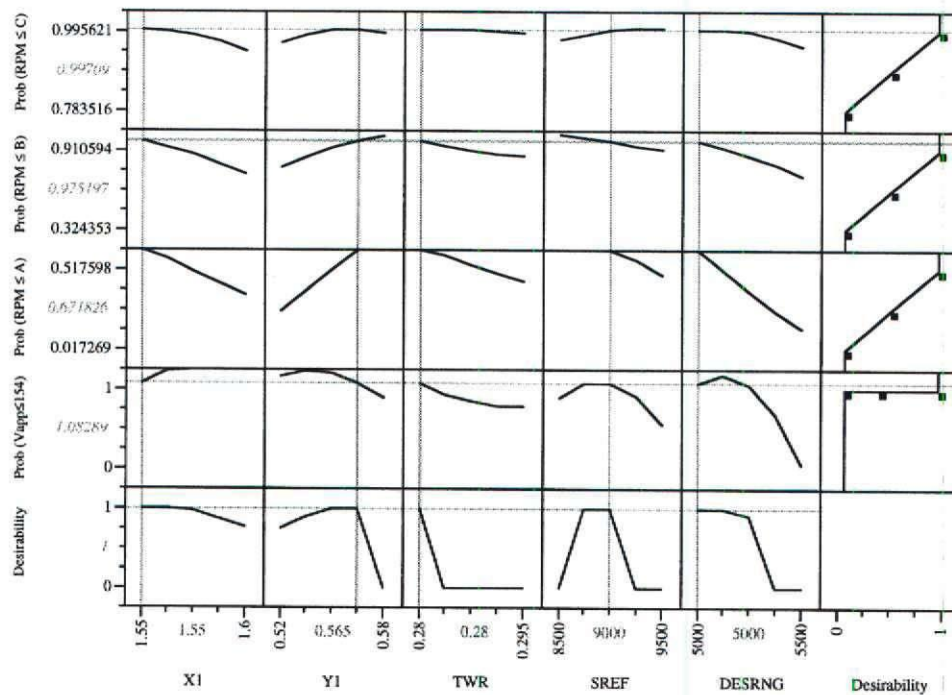
Figure 7. Prediction Profiles for Objective and Constraint Probabilities

The robust solution results as compared to the baseline HSCT are summarized in Table 4 and Figure 8. The table lists the five control variable settings associated with the robust solution as well as their baseline values. In the figure, for each target, the robust solution has a significantly higher probability of achieving the target. In fact, for the lowest target (target A), the baseline had a probability of zero. This graphic summarizes in a concise way the result of a RDS implementation.

Table 4. HSCT RDS Results- Mission Uncertainty Example

Control Variable	Baseline	Robust Solution
X1	1.615	1.55
Y1	.51	.565
TWR	.3	.28
Sref	8500 sq. ft.	9000 sq. ft.
DESRNG	5000 nm	5000 nm
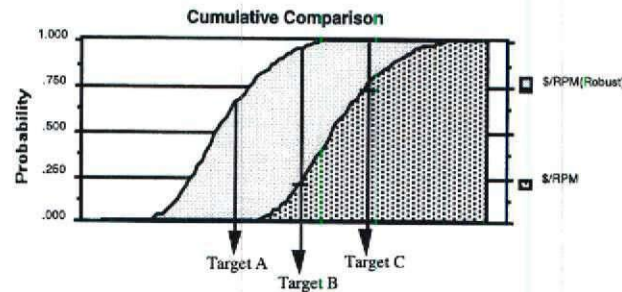
Figure 8. Cumulative Distribution Comparison- Mission Uncertainty Example

3.3. Disciplinary (Propulsion) Uncertainty with Disciplinary RSEs

Disciplinary uncertainty, though different in character from economic or mission uncertainty, is treated essentially the same in the RDS method. It can come from a variety of sources, including analysis tool imprecision and lack of design knowledge in the early design phases. For instance, it is very difficult to capture all elements which contribute to a response in a single analytical model without making the model excessively complex. This is especially true of complex systems such as aircraft. As a result, most analytical have a certain degree of uncertainty inherent to them.

The second effect is the implicit uncertainty in design knowledge as a design progresses from the conceptual to preliminary to detailed design stages. Typically, major design parameters such as wing area, thrust-to-weight ratio, etc. change somewhat as the design matures. This natural drift of system level parameters can be thought of as an uncertainty from a disciplinarian viewpoint.   For instance, the aerodynamicist whose job is to design a wing for optimum performance under some specified flight conditions is given wing area and loading targets from

conceptual analysis. However, as the design progresses through the preliminary stage, these targets may be somewhat modified due to results from disciplinary analysis in other areas such as structures or controls. The net result is uncertainty in design targets from an aerodynamics point of view.

Disciplinary uncertainty is also present all the way down to part-level design. A prime example of this can be found in design of combustor liner cooling systems in gas turbine engines. The flame temperatures found in modern gas turbine combustors is far above that of the melting temperature of the combustor materials, and it is therefore necessary to cool these parts to prevent premature and/ or catastrophic failure. Typically, combustors are cooled using compressor discharge air which is usually at a relatively cool 1200 F. The job of the combustor cooling designer is to design the combustor cooling system which uses the minimum amount of cooling air possible while simultaneously keeping the combustor cool enough to prevent failure, overheating, spilling, etc.

Combustor cooling efficiency is dependent on parameters such as compressor discharge temperature, flame temperature, and heat transfer convective coefficient on both the flame and coolant side of the combustor liner. Unfortunately, each of these parameters has a certain degree of associated uncertainty . For instance, compressor discharge temperature is dependent on flight condition, ambient conditions, compressor efficiency, seal wear, and many more parameters which are beyond the cooling designer's ability to control. Typically, the cooling system designer must proceed based on the predictions of an engine cycle analysis and try to design a cooling system based on a worst-case estimate of compressor discharge temperature.

Likewise, flame temperature also has some degree of associated uncertainty. First, the turbine inlet temperature (TIT) may change somewhat as the design progresses due to changes in design requirements of the engine. Second, flame distribution within the combustor volume is not uniform and it is typical to have zones where the flame temperature is higher than elsewhere. Finally, heat transfer coefficients have some degree of uncertainty due to non-uniformities in flow patterns within the combustor. For instance, some areas within the combustor are subjected to

intense flame scrubbing which increases the local heat transfer coefficient and results in "hot spots" in the combustor.

Taken together, these uncertainties in design parameters constitute a serious concern in the design of a combustor cooling system. Historically, the method used to overcome this uncertainty was to design to meet an assumed "worst case" condition. This sometimes resulted in overdesign of cooling systems which an attendant reduction in propulsive efficiency. However, for modern engines, every ounce of efficiency is of tantamount importance and the penalties associated with this "worst case" method are no longer acceptable. In the case of the combustor liner problem, environmental objectives dictated that cooling air mass flow rate be minimized while simultaneously guaranteeing acceptable metal temperatures. The combustor configuration did not have sufficient design margin to use the "worst case" method and an alternative was needed.

A goal in the RDS setting is to find ways of quantifying this uncertainty such that the designer has the ability to design for uncertainty rather than resorting to a "worst case" method. The example of robust combustor liner design is a very detailed example of robust methods applied to the part level of a system [Ref. 7]. However, these methods apply equally well to all other levels of design detail.

3.3.1. Robust Liner Design Methodology

The objective of liner cooling design is to keep the liner peak metal temperature below some maximum metal temperature, set by strength and material considerations, using the smallest cooling mass flow rate possible (material thermal stress considerations are not considered at this point). In addition, since an LPP combustor must use minimal liner cooling flow, there is little design margin available to compensate for uncertainty in the analysis process. Thus, the designer needs a way of minimizing the effect of uncertainty in such a manner as to be reasonably assured that liner temperature limitations will not be exceeded regardless of flight condition, ambient temperature, manufacturing imperfections, and so on.

3.3.2. Liner Cooling Model

A step-by-step description of robust cooling design methodology is given in Figure 9. The central element is an analysis tool that is capable of predicting the peak liner metal temperature as a function of cooling geometry, liner flame (gas) side boundary conditions, and liner backside (coolant-side) boundary conditions (depicted inside the dashed box in Figure 9). Backside boundary conditions are calculated through cycle analysis and cooling analysis. Cycle analysis is used to calculate coolant temperatures (T_3) while cooling analysis is used to calculate backside heat transfer coefficient. Typically, this cooling analysis is based on a regression of experimental data for the cooling configuration under consideration.

Flame-side (or gas side) boundary conditions are more difficult to calculate because flame side flow patterns are usually not uniform. Those zones near a swirler cup are subject to intense flame scrubbing which creates hot-spots in the liner material. In addition, the calculation of radiative heat flux into the liner walls is a very difficult task and typically consists of a considerable amount of guesswork on the designer's part. Finally, it is usually necessary to use CFD analysis in order to get a reasonably accurate estimation of the boundary conditions along the wall. Lacking this, one must at least have some idea based on historical knowledge of what typical values for convective heat transfer coefficient and adiabatic wall temperature are for the configuration under consideration.

The liner thermal model and boundary condition calculation routines collectively constitute a mathematical model for liner metal temperature as a function of cycle parameters and cooling system geometry. In an abstract sense, one can think of the liner cooling model as a "black box" which takes cooling geometry and cycle information and returns a liner metal temperature, as shown in Figure 9. Since several of the input parameters may be considered as noise factors, the model has some inherent uncertainty in the calculation of liner temperature.

1. Start with Design Variables of Interest, Create Screening Test Using DoE

2. Analyze Each Case in Liner Impingement Model to Find Resulting Metal Temperature

3. Fix Variables that are Insignificant to Liner Temperature. Create RSE for Liner Temperature as a Function of Remaining Design Variables

4. Assign Distributions to Noise Parameters; Use RSM to Create an RSE of Mean Temp & Variance as a Function of Control Variables

5. Define OEC=Mean*Var; Optimize for Minimum OEC Using Classical Techniques

Figure 9. Robust Combustor Liner Cooling Design Methodology

3.3.3. Screening Test

The impingement model consists of a set of nine input parameters and a single response, listed in Table 5. Three of these are impingement geometry parameters (x/D, Z/D, D) and two are engine cycle parameters (T_{flame}, T_{cool}). x/D is the non-dimensional impingement hole spacing, Z/D is impingement gap spacing, and D is impingement hole diameter. The parameter h_{gas} is the flame side convective coefficient, K is liner metal thermal conductivity, $\Delta P/P$ is impingement baffle pressure drop as a percentage of P_4, and TBC Thickness indicates the thickness of the TBC coat on the flame side of the liner. T_{flame} is the adiabatic flame temperature, and T_{cool} is the coolant temperature impinging on the liner backside (taken to be equal to compressor discharge temperature). Note that the design variables consist of three noise (denoted "N") and six control parameters (denoted "C").

Table 5. Screening Test Parameters and Ranges

Parameter	Units	Control/Noise
x/D	-	C
Z/D	-	C
D	in	C
T_{flame}	F	N
T_{cool}	F	N
h_{gas}	BTU/hr-ft2-F	N
K	BTU/ft-hr	C
ΔP/P	% P4	C
TBC Thickness	in	C

A minimum and maximum value was selected for each of the variables based on design experience, and a DoE used to set up a fractional factorial experiment consisting of 33 cases. For all cases, the value of each input parameter was set either to the max (+1) or min (-1) value with the exception of the last case, in which all inputs were set to the midpoint of each range. Due to the proprietary nature of these ranges, only the normalized (±1) values for each variable are presented here. Each case was run using the liner cooling model defined earlier to find the peak metal temperature in the liner. This data was then analyzed using JMP[9]. The results can be expressed in the form of a Pareto plot as shown in Figure 10.
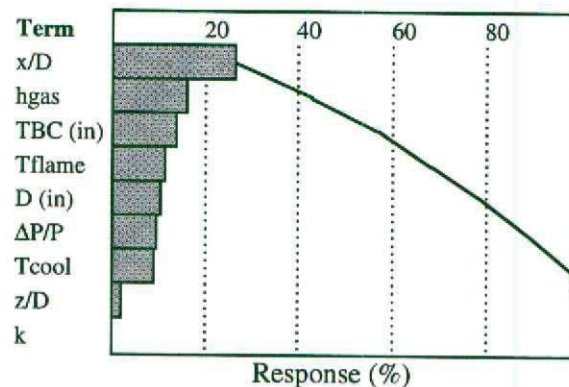
Figure 10. Pareto Plot of Liner Cooling Parameters

Once the number of important variables was identified, a so-called *disciplinary RSE* was generated for the liner temperature. This equation serves as a model which both relates the key

design parameters to the selected response and facilitates the implementation of RDS. This implementation is described next.

Once again Monte Carlo simulation is used to show the effect of uncertainty on the liner temperature. In order to do this, each of the noise parameters is given a fixed probability distribution based on design experience. After assigning fixed distributions to the noise parameters, it is possible to assess how the control parameters affect the mean and variance by simply changing the values for the control parameters and looking at the resultant mean and variance. Equations for liner temperature mean and variance are derived using RSM in the same fashion as for the liner temperature RSE before. Once again, DoE is used to design an experimental setup consisting of 27 cases in which each of the four control variables is varied between their minimum and maximum values.

Statistical analysis of the Monte Carlo simulation results shows that the hole spacing (x/D) and the TBC thickness have a strong effect on the temperature variance while the effect of pressure drop and hole size are small. Similarly, TBC thickness and hole spacing have a strong effect on liner mean temperature. This trend is reflected in the Pareto plots of Figure 11. Note that the liner temperature variance is dominated by the first two terms, whereas the mean temperature must include at least the first 4 terms in order to get a reasonable approximation of the response. Also, note that the interaction of x/D with itself is a significant factor in the determination of liner mean temperature.
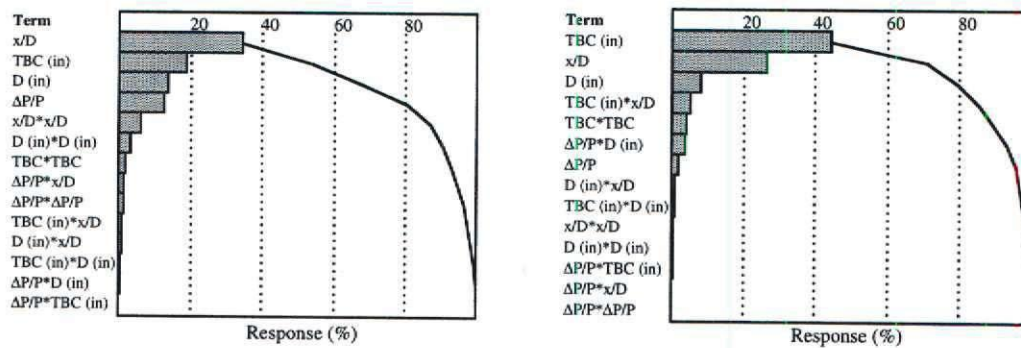
Figure 11. Pareto Plot of Combustor Liner Temperature (a) Mean and (b) Variance

These results can also be given in the form of prediction profiles as shown in Figure 12. The prediction profile is a matrix of plots showing each variable plotted against each response to show how the responses are effected by each parameter over the ranges investigated. The prediction profiles also give the designer an estimate of response sensitivities. A steep profile indicates the response is highly sensitive to that input, while a flat line indicates the input has no effect on the response. These results were subsequently used to generate a robust design based the OEC in Equation (1), since this particular example was conducted before the transition to the probability minimization objective illustrated in the two previous examples.
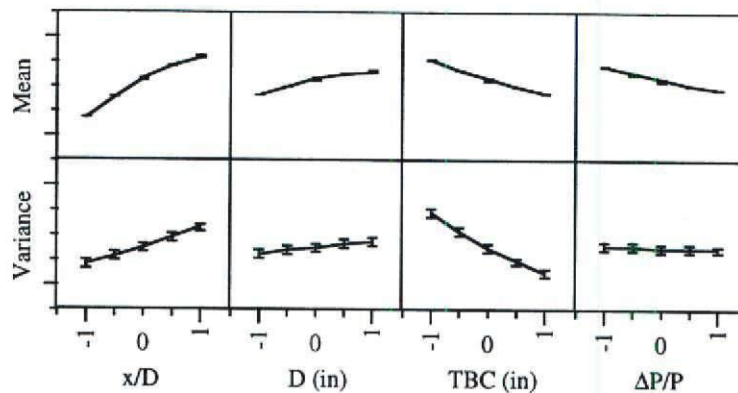
Figure 12. Prediction Profiles for Combustor Liner Mean Temperature and Variance

3.4. Disciplinary RSE- Structures

The goal of this example is to generate an RSE for wing structural weight for an HSCT-type aircraft. It is part of the overall classroom case study described in the Introduction of this report to completely perform this task a number of steps have to be taken, the first of which is the construction of a detailed structural model of the wing. Next, aerodynamic and thermal loads must be applied to this model. These loads, in turn, must either be calculated internally by the structural analysis code or imported by an external aerodynamics code. Finally, this model under load is analyzed subject to a set of constraints such as stress, flutter, and deflection. The thickness of the model elements must then be sized to meet these constraints, yielding an optimized structural wing weight.

This process must then be repeated in a systematic manner for different design variable values, as assigned by a DOE. Generating a weight response for each case according to the DOE matrix will then yield a quadratic equation of wing weight as a function of the chosen design variables. Figure 13 visually illustrates the iterative process to develop a wing weight equation.
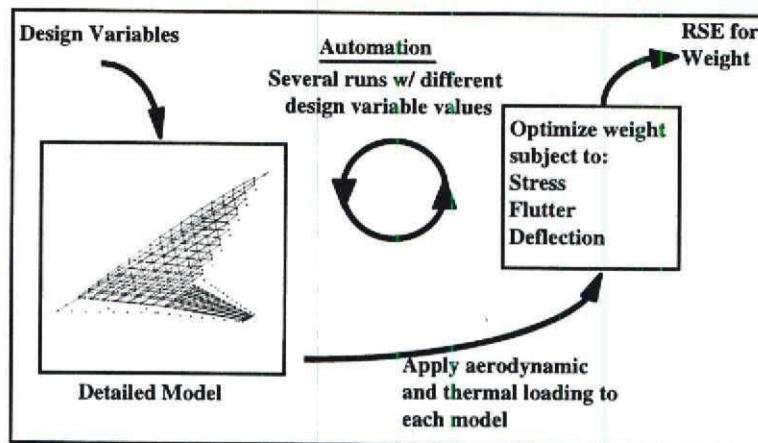
Figure 13. Wing Weight Generation Process

Two structural analysis codes, both of which have been used in the ASDL, were studied as possible candidates as the structural tool for this study. The first of these is the Equivalent Laminated Plate Solution (ELAPS). The second is the Automated Structural Optimization System (ASTROS). ASTROS was chosen as the tool to be used in this study despite the complexity and steep learning curve associated with it. The primary reason for choosing ASTROS over ELAPS is its power as a structural analysis and design code, including its ability to perform flutter analysis and optimize wing weight. Additionally, its ability to model aerodynamic loads internally was attractive, especially since the alternative was to import loads from an external source if ELAPS were used. However, ELAPS remains a viable option for structural analysis within RDS if ASTROS proves to be inappropriate.

3.4.1. ASTROS

ASTROS was developed by the Flight Dynamics Directorate, Air Force Wright Aeronautical Laboratory, and has many favorable attributes for this study despite a steep learning curve. ASTROS combines finite-element based structural analysis, aerodynamic analysis and optimization algorithms, making it a complete structural design tool. The finite-element analysis subroutines are capable of stress, modal and thermal analysis. The aerodynamic analysis uses USSAERO for steady aerodynamics and Doublet-Lattice and constant pressure methods for unsteady aerodynamics. ASTROS can optimize a structure subject to many different constraints, typically minimizing structural weight by optimizing element thickness subject to a particular constraint. It can be used to model the entire aircraft including the fuselage, empennage and landing gear. ASTROS is much more than a conceptual design tool and is capable of doing analysis in all phases of the design process.

In spite of its many advantages as a complete design tool, the use of ASTROS does have a cost. It is difficult to automate which is very important when implementing the RSM. In addition, it has a high computational cost for a complex model. Time to both learn and implement the code is the most significant factor when using ASTROS in the design process.

The construction of the FEM was also facilitated by a mesh generator, developed in "in house" at ASDL. This mesh generator has the capability to create an ASTROS input file for an HSCT of arbitrary planform given wing geometry parameters. Since RSM requires numerous runs of varying configurations, the mesh generator is an invaluable tool that allows quick generation of many different configurations in minimal time.

3.4.2. Assumptions

Chief among the assumptions is that of using a simplified representation of the wing as shown in Figure 14. Specifically, the task of modeling detailed internal wing geometry in ASTROS is a long and laborious process and would have taken far to long to complete for this Year one effort. Therefore, the wing was modeled as a flat plate comprised of all-titanium quadrilateral elements (See Table 6. Titanium Material Allowables, CQUAD4 in ASTROS Bulk Data). In this representation, the wing is divided into seven regions as shown in Figure 14. The first three regions are structural regions, and the last four are flaps.

Table 6. Titanium Material Allowables

Titanium (Ti6-Al-4V) Material Allowables	
$\sigma_{allow\ (tension)}$	$0.104*10^8$ lb/ft^2
$\sigma_{allow\ (compression)}$	$0.104*10^8$ lb/ft^2
$\sigma_{allow\ (shear)}$	$0.608*10^7$ lb/ft^2
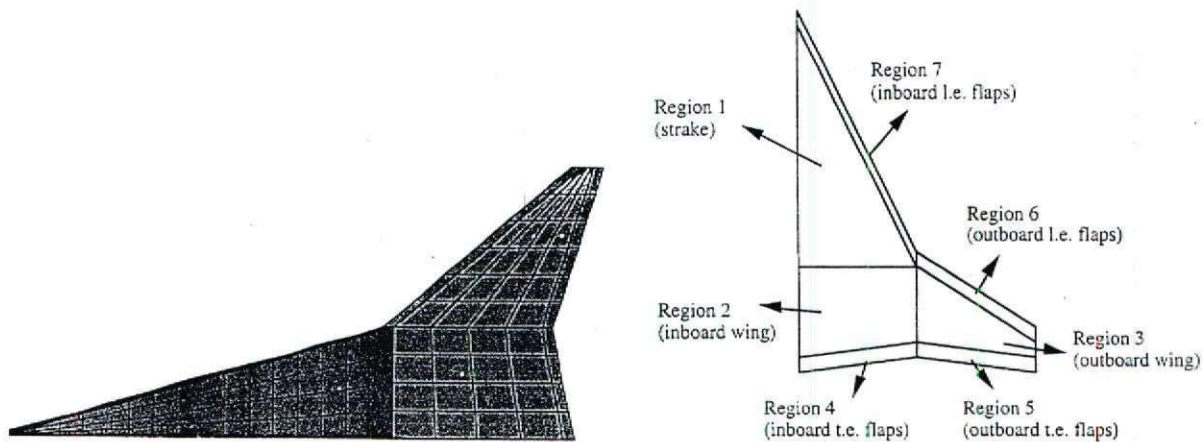
Figure 14. Representation of Wing and Wing Regions

Wing strength was tailored to meet a specified sizing maneuver. Though a number of maneuvers (symmetric and asymmetric) and load conditions (2.5g, -1g) should be considered in the structural sizing process, due to time limitations only one maneuver could be considered. Previous research conducted on HSCT Structural concepts by Lockheed [Ref. 8] found that one maneuver was primarily the most critical. This maneuver was a symmetric +2.5g pull-up at Mach 0.9 and 35,000 ft.

Fuel in the wing was modeled as concentrated mass at each of the nodes internal to the leading and trailing edge. From a baseline FLOPS file a wing fuel weight of 400,000 lbs. was assumed for the entire wing (200,000 lbs. for half-wing). Of this weight, 33% was placed in the strake region, 45% in the inboard wing box, and 22% in the outboard wing box.

The engines were modeled as lumped masses with an approximated weight of 21,000 lb. per engine. The engine nodes were "attached" to the rest of the structure using multi-point constraints. These constraints dictate the motion of the engine node by constraining the deflection of the node to be dependent on the deflections of the nodes surrounding it. It was initially hoped that engine location could be a design variable in the weight RSE. However, time limitations once again forced the location of the engines to be fixed at their baseline values (19.407 ft from A/C center for inboard engine, and 32.3 ft from A/C center for outboard engine). Future studies may

wish to examine the impact of engine location on wing weight, since its contribution could be significant to the aeroelastic performance of the wing.

3.4.3. RSE Results

In any RSM exercise, one of the first procedures is to define the design variables and ranges (design space) to be used in creation of the RSE. The ranges correspond to the minimum and the maximum values of the design variable. The 9 original design variables and their values are shown in Figure 15. TOGW was added since the weight of the aircraft directly determines the loads on the wing, and thus has a tremendous impact on the required thickness of the structural members.

Variable	Description	Min. Value	Max. Value
X_1	LE Kink	1.54	1.69
X_2	LE Tip Location	2.10	2.36
X_3	TE Tip Location	2.40	2.58
X_4	TE Kink Location	2.19	2.36
X_5	TE Root Location	2.19	2.50
Y_1	Y Kink	0.44	0.58
S_{wing}	Wing Area (ft²)	7800	8800
TOGW	Takeoff Gross Weight (lb)	750,000	1,000,000
T_{lb}	Equivalent Inboard Thickness (ft)	0.16	0.29
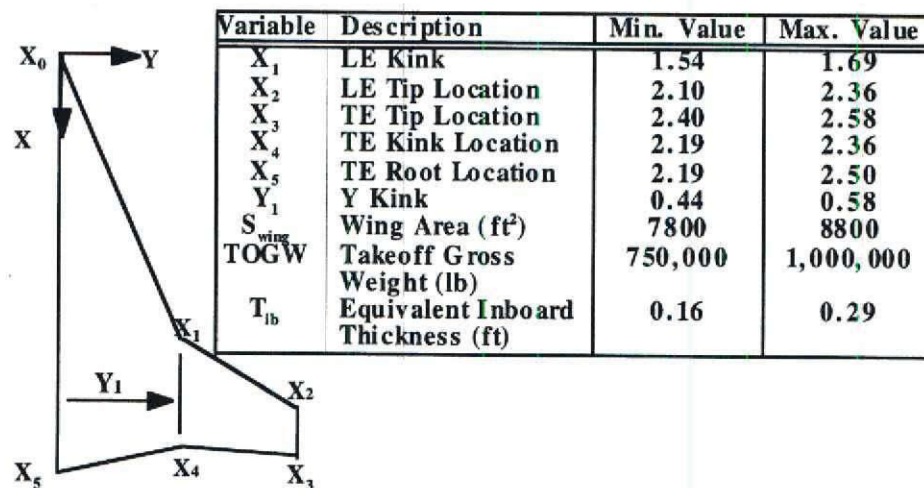
Figure 15. Design Variable Definition and Ranges

With the design variables and their ranges defined, the next step was to find stress critical elements in the FEM. This was accomplished by examining a number of different wing configurations at different TOGW, and observing which panel elements in the wing consistently had the highest Von-Mises stresses. Figure 16 shows 6 panels that had high stresses for all configurations. However, for every configuration examined, one of the root panels (46,47, or 48) always contained the highest stresses, and thus were identified as stress critical panels that would be monitored in the following screening test and stress RSE determination. The kink panels

(78,79,80), though never observed to be stress critical in the cases that were examined, always had high enough stress to warrant their inclusion as responses in the screening test and stress RSE.
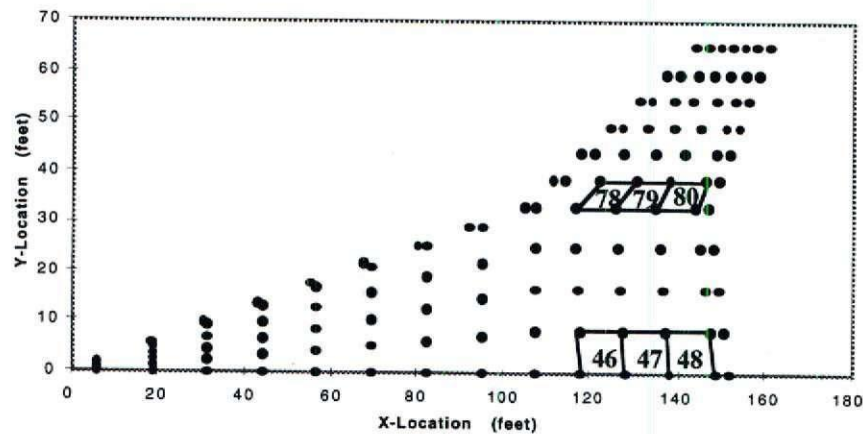
Figure 16. The Stress Critical Elements

The design space of the stress response is defined nine variables. The first step taken was to use a screening test to determine which variables contributed the least to the response. Ideally, the number of variables should be reduced to eight or less to reduce the number of cases for the RSE generation. The screening test response is Von-Mises stresses at each stress critical panel, and the DoE setup employed is a 2-level Resolution-IV Fractional Factorial DoE for 9 factors (64 cases). The effect of each design variable on the Von-Mises stress response for the three root panels is visually illustrated in the form of Pareto plots in Figure 17. It is clear from these plots that the variables S_{wing} and X_3 contribute the least to the stress response, and thus were fixed to their baseline values for the RSE phase to 8100 ft^2 and 2.49, respectively.

Term	Scaled Estimate	.2 .4 .6 .8
Inboard Thickne	-0.5519596	
TOGW	0.44921455	
X5	-0.1199174	
X1	0.11212257	
Ykink	0.08080667	
X4	-0.053489	
X2	0.02692631	
Swing	-0.0161114	
X3	-0.0158784	

Element 46

Term	Scaled Estimate	.2 .4 .6 .8
Inboard Thickne	-0.6338962	
TOGW	0.49472487	
X5	-0.1901304	
X1	0.11356708	
Ykink	0.08583463	
X2	0.06503893	
X4	-0.0392957	
Swing	-0.0197691	
X3	-0.0162873	

Element 47

Term	Scaled Estimate	.2 .4 .6 .8
Inboard Thickne	-0.6803079	
TOGW	0.49146039	
X5	-0.3668102	
X2	0.09402252	
X1	0.09179813	
Ykink	0.08182875	
X4	0.05330812	
Swing	-0.0242207	
X3	-0.0109309	

Element 48

Figure 17. Pareto Plots from the Screening Test for the Von-Mises Stress

With the design space now reduced from 9 factors to 7 factors, 100 cases were set up according to a 5-level Central Composite DOE with 22 center points. The Von-Mises stresses were recorded for each case, and an analysis of variance was performed on the resulting responses to produce an RSE for Von-Mises stress at each of the stress critical panels. Figure 18 shows prediction profiles of the stress RSE for each of the root panels. Note that inboard wing thickness has the largest effect on node stress, as expected.
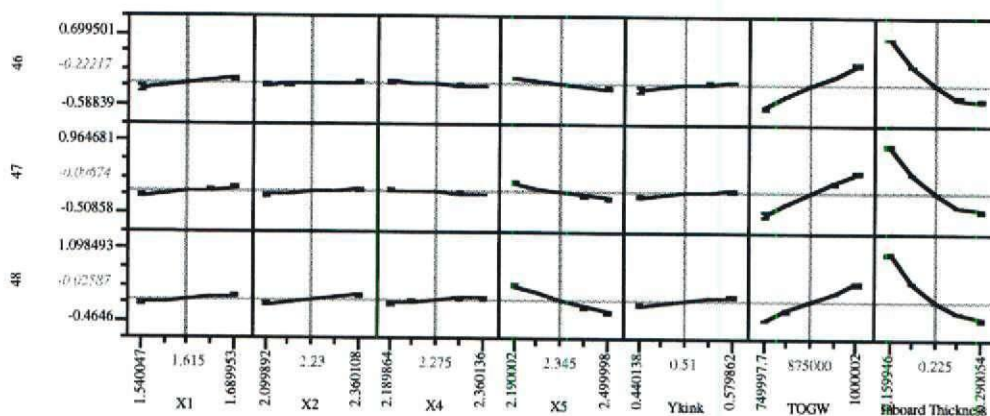
Figure 18. Stress RSE Prediction Profiles

The coefficients (b_i, b_{ii}, b_{ij}) of the resulting stress RSE's were then imported to an EXCEL spreadsheet which, setting the Von-Mises response to zero in the RSE and using the quadratic formula, would calculate inboard wing box plate thickness (T_{ib}) as a function of the design variables. Table 7 shows a sample of this Excel worksheet where **t** represents the inboard wing box plate thickness, **A1** is area of the strake, **A2** is the area of the inboard wing box, and **A3** is the area of the outboard wing box.

Table 7. Sample of Excel Worksheet

| X1	X2	X3	X4	X5	Ykink	Swing	TOGW	Semispan	A1 (ft^2)	A2 (ft^2)	A3 (ft^2)	t (in)
1.593	2.191	2.463	2.250	2.299	0.489	8151.4	837837	65.15	1653.54	1351.53	940.30	0.152
1.593	2.191	2.463	2.250	2.299	0.489	8448.7	912163	66.33	1713.85	1402.00	975.82	0.166
1.593	2.191	2.463	2.250	2.299	0.531	8151.4	912163	63.76	1718.69	1403.34	826.12	0.169
1.593	2.191	2.463	2.250	2.299	0.531	8448.7	837837	64.92	1781.37	1455.77	857.35	0.154
1.593	2.191	2.463	2.250	2.391	0.489	8151.4	912163	64.40	1615.60	1413.32	917.96	0.155
1.593	2.191	2.463	2.250	2.391	0.489	8448.7	837837	65.56	1674.52	1466.02	952.65	0.142
1.593	2.191	2.463	2.250	2.391	0.531	8151.4	837837	63.00	1677.73	1466.22	805.72	0.145
1.593	2.191	2.463	2.250	2.391	0.531	8448.7	912163	64.14	1738.92	1520.93	836.20	0.158
1.593	2.191	2.463	2.300	2.299	0.489	8151.4	912163	64.31	1611.09	1367.21	968.76	0.167
1.593	2.191	2.463	2.300	2.299	0.489	8448.7	837837	65.47	1669.85	1418.23	1005.30	0.153
1.593	2.191	2.463	2.300	2.299	0.531	8151.4	837837	62.98	1676.38	1421.22	852.13	0.155
1.593	2.191	2.463	2.300	2.299	0.531	8448.7	912163	64.11	1737.52	1474.29	884.29	0.170

Since thickness of the inboard wing box can now be found for any combination of the design variables (within their respective ranges), total wing weight can be calculated. Material density is required to calculate the weight of the wing. However, since the flat plate model neglects the space that would exist between the skin panels of a real wing, if the actual density of titanium were used, the wing weight would be unrealistically heavy. To account for this limitation in the flat plate model, a reduced density based on structural densities from the Lockheed [Ref. 8] study is used to 'capture' the space between the skin panels for each structural section. The reduced densities used for each section are:

$$\rho_{strake} = 47.1 \text{ lb/ft}^3$$

$$\rho_{ib\ wing} = 51.9 \text{ lb/ft}^3$$

$$\rho_{ob\ wing} = 63.9 \text{ lb/ft}^3$$

and as a comparison:

$$\rho_{titanium} = 276 \text{ lb/ft}^3$$

With the capability to determine wing weight using the Excel spreadsheet for any point in the design space, a third DoE is set up, this time with wing weight as the response and 8 design variables (X_1 - Y_1, S_{wing}, and TOGW) as the elements of the matrix. A 5-level 177 case Orthogonal Central Composite DoE with 33 center points was used, and an analysis of variance of the response according to the DoE produced the prediction profiles for each of the wing section weights shown in Figure 19.
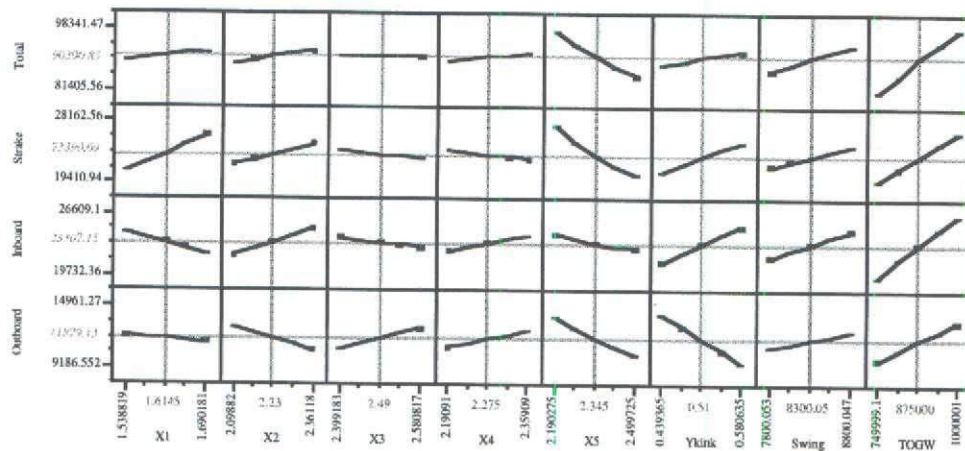
Figure 19. Wing Weight RSE Prediction Profiles

The fit of the RSE to the experimental data is captured by the R^2 value and the residual plot. For the wing weight RSE these are given in Figure 20 and indicate an acceptable fit.

Rsquare   **0.99887**
Mean   **90386.24 lb**
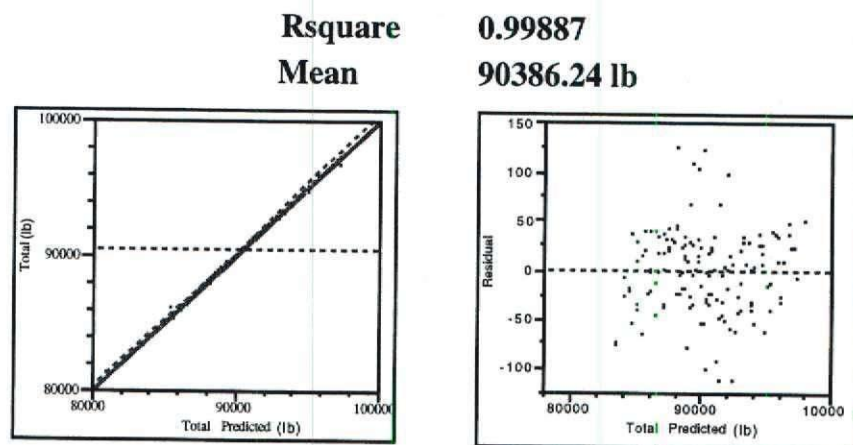
Figure 20. Fit of the Wing Weight RSE

As a tool for understanding the influences on wing weight, a Pareto plot was also generated for total wing weight (Figure 21) using all terms in the RSE, including the interacting effects. As clearly seen in Figure 21, over half the terms in the RSE have little to no effect on the total wing weight response. The most significant contributors (with the exception of X_3) are the first-order terms. This also is evident from the weight RSE prediction profile (Figure 19) in which the response is nearly linear with respect to the design variables.

Term	Scaled Estimate	
TOGW	2384.4264	
X5	-1638.1314	
Swing	987.4173	
Ykink	510.3777	
X2	498.1811	
X1	355.1787	
X4	270.2653	
TOGW*X5	-110.5411	
X5*X5	107.6660	
TOGW*TOGW	-62.0744	
TOGW*X1	41.0025	
TOGW*Swing	40.1835	
X5*X2	-38.8027	
TOGW*Ykink	32.9011	
Swing*X5	-28.1576	
X5*X1	-27.1582	
Ykink*Ykink	-23.6674	
X3	-21.8707	
X4*X2	15.2824	
Ykink*X2	-11.6929	
Swing*Ykink	8.4445	
Swing*X2	8.3827	
X4*X1	-7.6357	
X4*X4	-6.6718	
Swing*X1	6.1110	
TOGW*X4	5.5869	
X2*X1	5.5447	
X2*X2	-5.5279	
Swing*Swing	-5.4629	
X1*X1	-5.4405	
X3*X3	-5.3494	
Swing*X4	4.5056	
Ykink*X5	4.0608	
X5*X4	-3.6483	
Ykink*X4	-3.1155	
Ykink*X1	1.1810	
TOGW*X3	-0.8748	
Ykink*X3	0.8271	
X3*X2	-0.5684	
Swing*X3	0.5093	
X5*X3	0.3536	
X3*X1	0.1301	
TOGW*X2	0.0418	
X4*X3	-0.0072	

Figure 21. Wing Weight Pareto Plot

4.   Neural Networks and Fuzzy Logic:

Potential Improvements over RSM

Since the RSM uses a least squares approach to generally fit a quadratic function, there are some limits on the use of Response Surface Equations (RSEs):
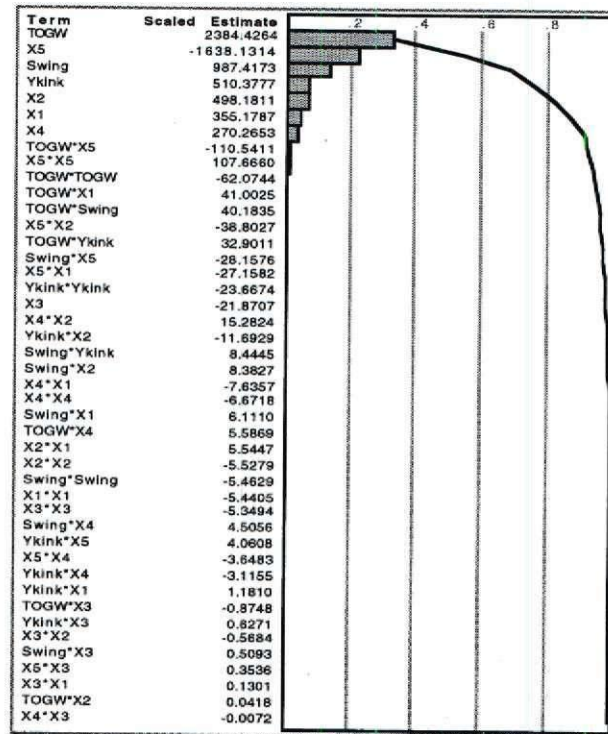
- The Response Surface Equation typically cannot handle more than 9 to 11 variables, which can mean enormous limitations especially in the case of such a complex system as an aircraft.

- The functional form of the RSE must be pre-specified; transformations are possible but not guaranteed to improve the prediction accuracy

- Even with very small ranges of the variables, the fit in some cases is still not satisfactory.

- RSM treats only continuous variables

All this calls for ways to approximate unknown functions in a different way. The object of this portion of the Year one effort was to identify, gather literature, and begin preliminary assessments of alternative methods of function approximation which are still applicable to the evolving design process. Two such methods identified and described next.

4.1. Neural Networks

A Neural Network is generally made up of many very simple processing units called neurons. Figure 22 illustrates such a processing element in the case where it has only one input.
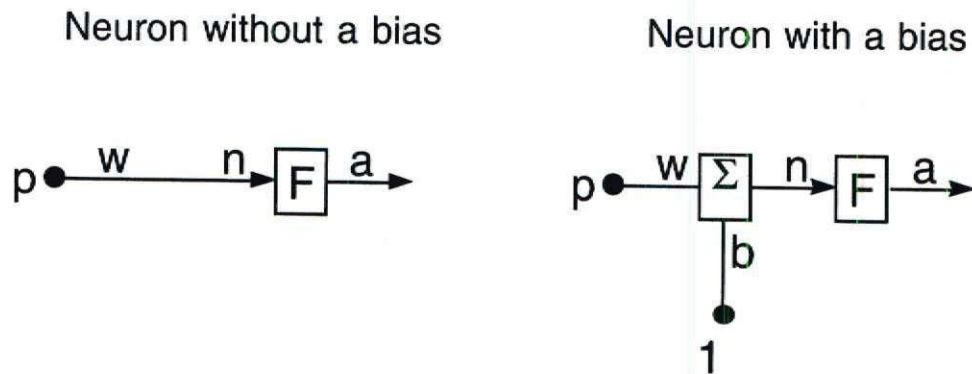
Neuron without a bias   Neuron with a bias

Figure 22: Single Input Neurons with and without a bias

Associated with each neuron is the transfer function with which it operates. n denotes the input to the transfer function F, and a is the output of the transfer function , which is also the output of the neuron itself. A neuron can work with or with out a bias. If there is no bias, the input p multiplied with the weight w forms the input for the transfer function f. Thus, the equation that relates the output to the input can be expressed as follows:

$$a = F(w*p)$$

If there is a bias, it is added to the weighted input term, before the term is entered in the transfer function. The equation to describe the operation the neuron fulfills would therefore be:

$$a = F(w*p + b)$$

The weight *w* and the bias *b* are adjustable parameters. The bias can be viewed as an additional weight, who's corresponding input is always 1. The advantages of using a bias is for one, that it is another parameter that can be adjusted to help train the network to give the desired values. Also, a bias is often necessary to be able to reach all the desired output values, since it creates the effect of an off-set.

4.1.1. Neuron with several inputs

A neuron with multiple inputs and a bias is shown in Figure 23. Here, there are R inputs and thus R weights involved. The input n for the transfer function is formed by multiplying each input, p(k), with its corresponding weight, w(1,k), where k = 1,2,...,R, and then adding the bias. The first index of the weight indicates the number of this neuron, for the case that there may be more than one neuron in this layer. (See next section)
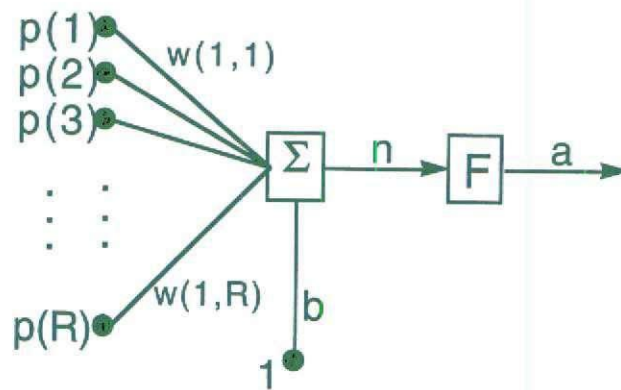
[From: MATLAB, NN toolbox[Ref. 9]]

Figure 23: Neuron with multiple inputs

In this case the vector of inputs and the vector of weights are:

$$w = [\, w\,(1,1) \;\; w\,(1,2) \;\; ... \;\; w\,(1,R)\,] \qquad p = \begin{bmatrix} p(1) \\ p(2) \\ p(3) \\ . \\ . \\ . \\ p(R) \end{bmatrix}$$

Then the input n for the transfer function is made up of the dot product of the weights and input vectors and of the bias:

$$a = F (w*p + b)$$

4.1.2. A Layer of Neurons

In Figure 23 a layer of Neural Networks is depicted. Here, there are R inputs and S outputs. The number of outputs is equal to the number of neurons in the output layer (the last layer).
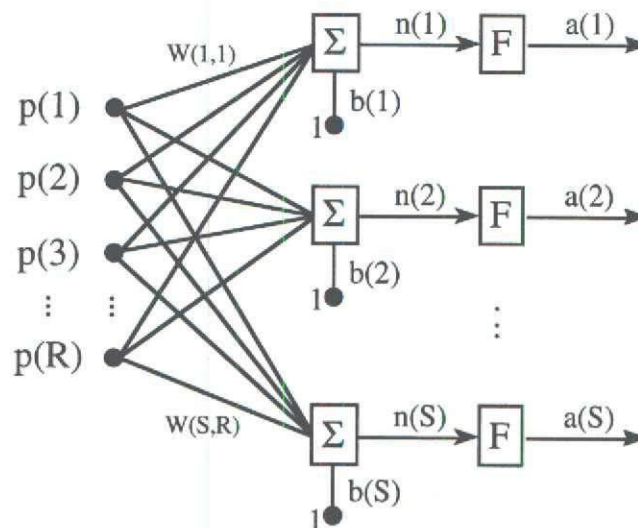
[From: MATLAB, NN toolbox[Ref.   9]]

Figure 24: Layer of Neurons

The transformation the network performs can then be described in matrix form as:

$$a = F (W*p + b)$$

It is clear, that now the output a and the bias b are vectors with S elements and the weights form a matrix with S rows and R columns. Equations for the separate outputs could be extracted from the matrix equation.

4.1.3. Multi-layer Neural Networks and Network Architectures

A Neural Network with three layers is shown in Figure 25. In a feed forward network, the outputs of the previous network layer are simply the inputs for the next layer until the last one is reached.

$$a1 = F1 (W1*p+b1)$$
Hidden Layer #1

$$a2 = F2 (W2*a1+b2)$$
Hidden Layer #2

$$a3 = F3 (W3*a2+b3)$$
Output Layer
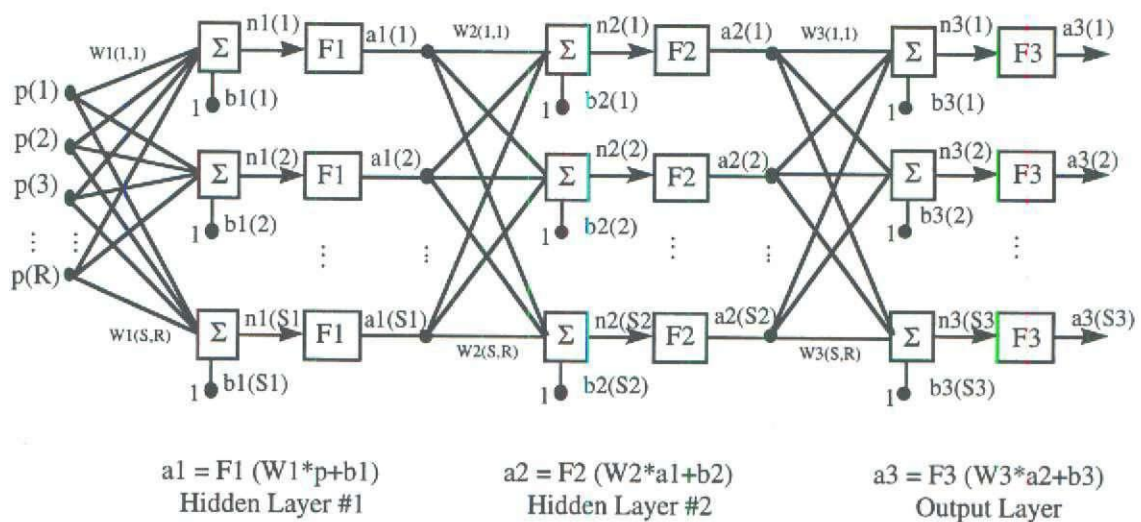
[From: MATLAB, NN toolbox[Ref. 9]]

Figure 25 : Neural Network with three Layers

There now is a weights matrix for every layer. The last layer is called the output layer, and the previous ones are the hidden layers. Occasionally, the inputs are referred to as the input layer, which can lead to confusion, since a three layer network to someone who counts the inputs as a layer is something different that what is to someone who does not count the inputs. Here, the

inputs will not be counted as another layer. The number of neurons in the output layer is determined by the number of outputs. The number of neurons in the hidden layers however is free and can be chosen.

4.1.4. Transfer functions

In principle, any function can serve as a transfer function. Some widely applied transfer functions are hardlimit , linear and sigmoid functions. Figure 26 and Figure 27 illustrate the graphs of these functions.
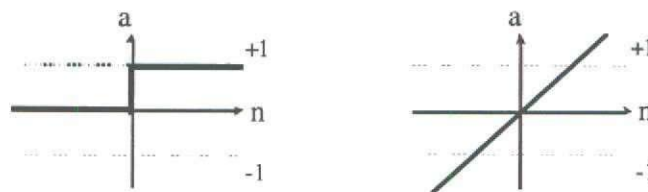
Figure 26: Hard Limit and Pure Linear Transfer Function
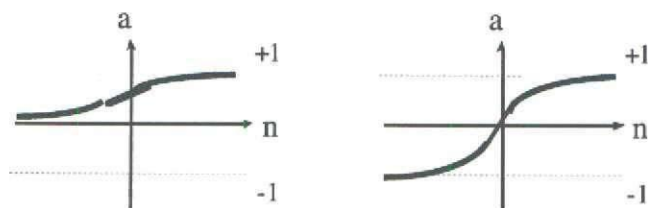
Figure 27: Log-Sigmoid and Tangent Sigmoid Transfer Function

4.1.5. Types of Neural Networks

There are many different types of neural networks for a lot of different applications. These include perceptron networks, different types of recurrent networks, networks with instar and outstar neurons and self-organizing maps. For the application in the IPPD design methodology as a method of function approximation, only the feed forward neural networks are of interest. Therefore, this report will focus on the function approximation with feed forward networks.

4.1.6. Function Approximation with Feed Forward Networks

The architecture of a feed forward neural network is usually a multilayer network as already shown in Figure 25. For each layer, there is a weights matrix and a vector of biases. These, together with the information of which transfer function is used in each layer, determines the neural network.

When evaluating the network answer for a certain input vector, there will be an answer a for each layer. The answer vector of the first layer will be serve as the input vector for the second layer, the answer of the second layer will be the input for the third, if there is one, and so on until the last layer is reached. Its answer will then be the total network answer. In this study, only networks where all the neurons in one layer have the same transfer function are considered. Also, it is assumed, that all neurons of each layer are connected with each neuron in the adjoining layers. Other constructions are possible, but they are not within the scope of this study.

4.1.6.1. Transfer Functions

A two layer neural network, with a hidden layer of neurons and an output layer, which has a tangent sigmoid transfer function in the hidden layer and a pure linear one in the output layer is known to be able to approximate any function arbitrarily well if there are enough neurons in the hidden layer. Such a network is depicted in Figure 28.

$$a1 = \text{tnasig} (W1*p+b1) \qquad a2 = \text{purelin} (W2*a1+b2)$$
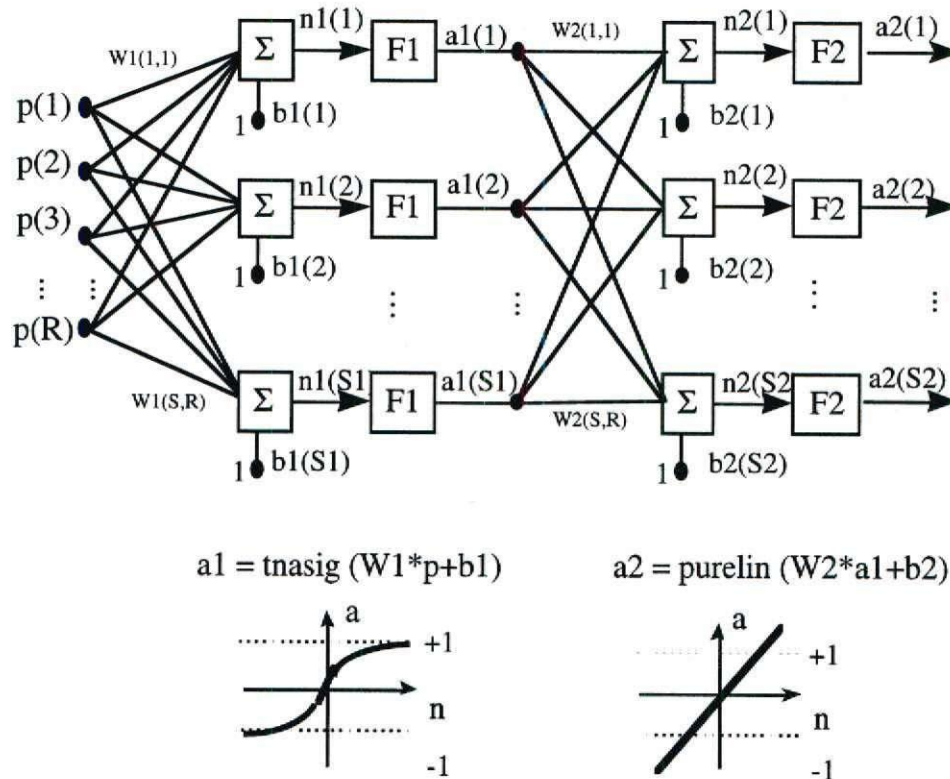
[From: MATLAB, NN toolbox[Ref. 9]]

Figure 28: Feed Forward Neural Network for Function Approximation

The sigmoid function is needed to introduce an effect of non-linearity. Otherwise, the network can only be able to simulate linear functions. It needs to be s tangent sigmoid function, since the logarithmic sigmoid only maps to positive values. The linear transfer function in the output layer is used to achieve outputs beyond the interval from -1 to 1. The tangent sigmoid layer maps the inputs to the interval between -1 and 1 and the pure linear function in the output layer can spread it over the entire range of the real numbers.

The following figures show the equations, by which this network is represented.

$$\begin{bmatrix} n1(1) \\ n1(2) \\ \cdot \\ \cdot \\ n1(S1) \end{bmatrix} = \begin{bmatrix} W1(1,1)\ W1(1,2)\cdots\ W1(1,R)\ b1(1) \\ W1(2,1)\ W1(2,2)\cdots\ W1(2,R)\ b1(2) \\ \vdots \qquad \vdots \qquad \vdots \qquad \vdots \\ W1(S1,1)W1(S1,2)\cdots\ W1(S1,R)b1(R) \end{bmatrix} * \begin{bmatrix} p(1) \\ P(2) \\ \cdot \\ \cdot \\ P(R) \\ 1 \end{bmatrix} \quad ; \quad \begin{bmatrix} a1(1) \\ a1(2) \\ \cdot \\ \cdot \\ a1(S1) \end{bmatrix} = \begin{bmatrix} tanh(n1(1) \\ tanh(n1(2) \\ \cdot \\ \cdot \\ tanh(n(S1) \end{bmatrix}$$

Figure 29: Matrix Equation for the First Layer (Tangent Sigmoid)

$$\begin{bmatrix} n2(1) \\ n2(2) \\ \cdot \\ \cdot \\ n2(S) \end{bmatrix} = \begin{bmatrix} W2(1,1)W2(1,2)\cdot\ W2(1,S)b2(1) \\ W2(2,1)W2(2,2)\cdot\ W2(2,S)b2(2) \\ \vdots \qquad \vdots \qquad \vdots \qquad \vdots \\ W2(S2,1)W2(S2,2)\cdot\ W2(S2,S)b2(S) \end{bmatrix} * \begin{bmatrix} a1(1) \\ a1(2) \\ \cdot \\ \cdot \\ a1(S) \\ 1 \end{bmatrix} \quad ; \quad \begin{bmatrix} a2(1) \\ a2(2) \\ \cdot \\ \cdot \\ a2(S) \end{bmatrix} = \begin{bmatrix} n2(1 \\ n2(2 \\ \cdot \\ \cdot \\ n2(S) \end{bmatrix}$$

Figure 30: Matrix Equation for the Second Layer (Pure Linear)

4.1.6.2. Training the network

The network is first initialized with random weights and then trained to represent the assigned problem. This is done by applying the a training values, of which input and outputs are known, to the network. Then with respect to the error, the inputs and the transfer functions used the network weights are change such that the error decreases. This is done repeatedly until the network error meets or is less than a previously selected error goal.

A set of training values consists of an input vector p and the target vector t that goes with it. First, the input p is applied to the network and the network answer a is calculated for this input. The total network error is defined as:

$$e = t - a$$

Then the weights change matrix for each layer is calculated according to the learning rule and using backpropagation.

4.1.6.3. Learning and Backpropagation

A simple and widely used learning rule is one using a plain gradient approach. It should serve as an example here to explain the learning and training process as well as the backpropagation.

For backpropagation, so-called deltas are calculated for every layer. For the output layer, which in our case is the second layer, the calculation looks like this:

$$d_2 = \frac{dF}{dn} * e$$

To calculate the delta for the first layer, the total network error is replaced by the delta of the second layer:

$$d_1 = \frac{dF}{dn} * d_2$$

The elements of the weights change matrices are:

$$dW_2 = d_2 * a_1 * lr$$

$$db_2 = d_2 * 1 * lr$$

$$dW_1 = d_1 * p * lr$$

$$db_1 = d_1 * 1 * lr$$

where lr is the learning rate. It has to be chosen with care; if it is too large, the network may 'jump over ' minima during the learning process, and the error will increase; if the learning rate is chosen very small, however, the network will converge very slowly. The ability to select a learning rate is governed by experience and does not have standard guidelines.

The new weights are obtained by simply adding the weights change matrices to the weights matrices:

$$W_1 = W_1 + dW_1$$

$$b_1 = b_1 + db_1$$

$$W_2 = W_2 + dW_2$$

$$b_2 = b_2 + db_2$$

The basic gradient approach backpropagation can be described as follows:

$$\Delta W(i, j) = lr*d(i)*p(j)$$

where, as previously discussed, p is the input vector to the current neuron layer, and d is the delta of that layer.

4.1.6.4. Batching

When multiple input and their associated target vectors are available, the inputs and the target vectors each form a matrix. The matrix of inputs P has is a (R,Q) dimensional matrix, where R is the number of inputs and Q the number of cases, for which data is available. The matrix of target values T is (S2,Q) dimensional, where S2 is the number of neurons in the second layer or number of outputs. The network answer of the first layer A1 is (S1,Q) dimensional, with S1 being the number of neurons in the first, the hidden layer. The answer of the second layer, which is the network answer A2 has the same dimensions as the target value matrix, and so does the matrix of errors.

All the equations can be applied to matrices too, such that all available training vectors can be applied at the same time. This is done repetitively until the total network error is below a certain error criterion.

4.1.6.5. Different Learning Rules and Training Methods

In addition to the training method based on the plain gradient approach discussed earlier, there are some other rather common training methods that should be mentioned here. A derived approach is the learning with momentum. Here a momentum constant is used to take the previous weight change into account. This then and the change is suggested by the basic gradient learning rule forms the new weights change. The equation that describes this methods may look as follows:

$$\Delta W(i, j) = mc\,\Delta W(i, j) + (1 - mc) * lr * d(i) * p(j)$$

Where *mc* is the momentum constant. Because of this factor, the approach with momentum is not as likely to get trapped in a local minimum as the plain gradient approach is. There is also the possibility of using an adaptive learning rate. It is basically the same approach described above as the basic gradient approach, with the only difference that the learning rate changes.

Each iteration, the new weights are calculated with the current learning rate, and then the network error is computed. If the error increased, the learning rate is decreased, and new weights and the network error are computed again; if the error is still increased, the learning rate is further decreased. This goes on, until the new set of weights achieves a smaller network error than the previous weights did. In that case, the weights are updated and the learning rate is increased. The approaches using the momentum and adaptive learning rate can also be combined, and they usually show better and faster convergence than the approach using the plain error gradient does.

Another enhanced approached uses the Levenberg-Marquart Optimization. This can mathematically be described as follows:

$$\Delta W = (J^T J + \mu I)^{-1} J^T e$$

Where e stands for the error and J is the Jacobian matrix of derivatives. Training a neural network with this method is significantly faster than any of the others, but it also usually requires more memory.

4.1.6.6. Initial Results and Observations

Several example test cases were conducted using a neural network to form a functional relationship from a set of data (usually data from an existing DOE). Many of the different attempts showed how sensitive the convergence is to the scaling of the outputs. The results also seem to show that, although convergence may be possible, the network does not necessarily represent the problem sufficiently well. It is also remarkable that those responses that did not fit well when their network was tested also took a long time to converge and converged only with a relatively high number of neurons. This suggests that the actual function may be a very complicated one, and it obviously is not captured by the constructed network.

At this point, a two layer neural network with a tangent sigmoid transfer function in the first layer and a linear transfer function in the second layer seems to be suitable to represent some of the responses. It is left to further investigations to find out why there were problems with other responses. Overall, there does not seem to be an inherent limit on the number of variables or their ranges as is the case with the Response Surfaces. This makes the application of neural networks in the IPPD design methodology seem highly favorable. This is the first study on this idea, and a lot of thought still has to be given to the details of implementing the neural networks in the methodology. Logical next steps include: search for and evaluate other possible learning rules and training methods that may be more suitable for complex systems, seek better ways of optimizing the number of neurons, research the impact of initial weights on the training, and examine the use of genetic algorithms to find the global optimum of the error surface with respect to the weights.
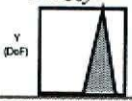
4.2. Fuzzy Logic

Fuzzy Logic systems can be used to represent nonlinear input/output relationships through the use of *if-then* rules. A noted attribute of FL is the simplicity of the models used to represent these

relationships as compared to other approaches. In reviewing literature for this report, FL applications included control system design of various types, pattern recognition, and function approximation. Certainly this is a mere subset of the variety of applications for which FL has been applied. Since the present focus is on function approximation, the reader should consult the references for further details on FL theory and its permutations [Ref. 10, 11].

In many FL scenarios, a human expert translates his or her knowledge of a problem to a series of initial *if-then* rules with the hope that these rules will form an adequate Fuzzy Inference System (FIS). FIS is the term for any system which uses fuzzy reasoning to map an input/output space [Ref. 12]. An example rule might be, "If (Wing Area is BIG) then (Gross Weight is BIG)". However, for less obvious situations or where the effects of parameter interactions are complex, sufficient human expertise may not exist which can create an initial FIS, let alone an effective one. A remedy proposed to deal with this dilemma is extracting the fuzzy rules from a set of input/output data (simulated or experimental) [Ref. 13].

Before discussing rule extraction, three basic types of FIS are identified. They are the Mandami, zero-order Seguno, and first-order Seguno. As Table 8 illustrates, the main difference between the three is how the output membership functions (MFs) are represented. These output MFs form the "then" part of the *if-then* rule sequence (also called antecedent-consequent pair)[5]. The antecedents are modeled by input membership functions. The input memberships functions *fuzzify* a crisp input by determining the degree of membership (between 0 and 1). For our previously defined example rule, the degree to which "Wing Area is BIG" may be defined as in Figure 31. This degree represents the amount of support for the rule which, when combined using an implication operator (such as min or max), form the output fuzzy set. This output set is modeled through the aforementioned output MFs. If the output MFs are fuzzy (Mandami FIS), they appear as distributions (one for each rule). The output is *defuzzified* by computing the centroid of the combined MFs. In the Seguno systems, the output is not a distribution by a single-valued MF (called a *singleton*). This facilitates defuzzification, which now consists simply of finding the weighted average of as many data points as there are rules.

Table 8. Types of Fuzzy Inference Systems (Y=output, X$_i$=inputs)

Type	Input MF's	Output MFs
Mandami	*Fuzzy (e.g. Fig. 1)*	*Fuzzy*
Zero-Order Seguno	*Fuzzy (e.g. Fig. 1)*	*crisp constant* $Y = k$
First-Order Seguno	*Fuzzy (e.g. Fig. 1)*	*crisp linear equation* $Y = k_o + k_1 X1 + k_2 X2 + ...$
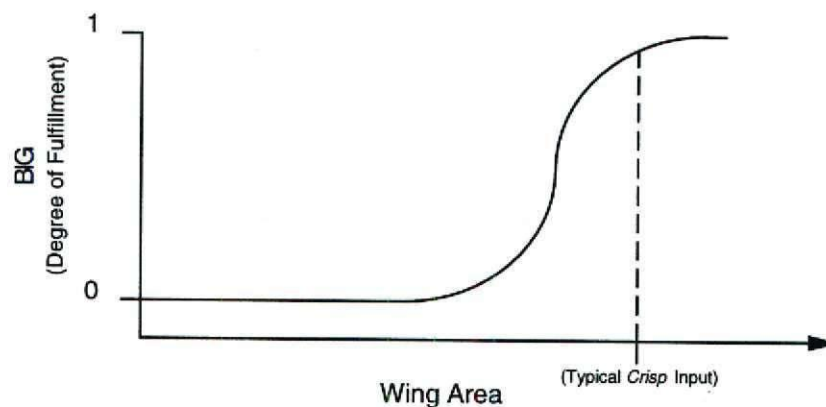
Figure 31. Example Input Membership Function (Antecedent): "If (Wing Area is BIG)"

Function approximation applications using FL proceed in two distinct steps. First, based on a set of input/output data, initial rules and their associated membership functions must be formulated in some way. The second step is to then tune the resulting FIS so as to obtain the desired prediction accuracy. With regards to step one, two techniques are readily available to form the initial FIS. One is a grid search technique, which, as the name suggests, simply partitions the data space in grid format and assigns rules accordingly. As a consequence, for systems with more than 4 or 5 inputs, this techniques becomes impractical due to the exponential growth of the number of rules with the number of inputs [Ref. 12]. The other method for distilling a FIS from a dataset is called clustering. In general, the clustering approach looks for patterns in the data (both input and output) and, once identified, takes advantage of these patterns by forming rules near the

point in the data space where large "mass" was found [Ref. 13]. Both methods are available in MATLAB. However, since the grid search technique suffers from the "curse of dimensionality" as the number of inputs increases, relatively large problems must be tackled with the clustering approach. In fact, it is in such problems with high dimensionality that the clustering algorithm is of increased benefit.

4.2.1. Initial Results and Observations

As an initial insight into the comparative strengths and weaknesses of FL and RSM, two example problems were investigated. The first was the prediction of a probability distribution for $/RPM from a previous study. The second related to a disciplinary model: approximation static pitching moment for a range of HSCT wing planforms. Fuzzy Logic and RSM estimators were formed in each case and resulted in the following observations.

• *Prediction Accuracy*: Based on the two example problems, there does not seem to be clear evidence that either FL and RSM is *always* more accurate than the other at representing a data space. The FL approach did seem to have an advantage when a relatively large set of data was available (the static pitch stability example), even under the circumstances of having 24% less training data points! The RSM fared better than FL with the small datasets of the probability prediction example.

• *Ease of Implementation*: In many respects, this issue is more a function of software design than anything inherent to the two theories. Once the data is generated, a useable FIS or RSE can be constructed about equally as quick (within minutes) using MATLAB and JMP© respectively.

• *Data Dimensionality*: Both methods have limitations in this area. RSM generally can be used to construct models (2nd order and above) of no more than 9 inputs. FL has no such

restriction per say, though the fitting ratio could quickly become unacceptable as the number of inputs grow. The clustering algorithm significantly extends the dimensionality allowed over the grid search technique, and thus, in certain situations, FL could be used for high dimensional cases out of reach of the RSM.

• *Reversibility/Differentiability*: This refers to the capability of switching an input to an output (and vice versa) in a function approximator. While an RSE is reversible (simply rearrange terms in the equation so that the variable of interest is isolated), it appears that one would have to start from scratch in the FL arena if an input/output switch is desired. In a related matter, an RSE can provide smooth derivatives in an optimization setting while such information in a FL setting would require finite differencing.

• *Functional Form*: Creating a RSE requires the assumption of a functional form (e.g. 2nd order polynomial, as was the case for the two examples here). Quick transformations are possible which allow the transition to a new form, though one might have to search among several possibilities before finding the best one. A FL predictor requires no *a priori* assumption in this way. Among the three types of FIS defined (see Table 8), the 1st-order Seguno has been mentioned in the literature as being the most accurate in almost all cases.

• *Discrete/Continuous Variables*: Both examples presented in this study consisted of continuous input and output variables. Many times, however, a need will arise to examine systems with a mixed continuous-discrete composition. The RSM is predicated on all input variables being continuous (since it seeks to construct continuous multidimensional surfaces to map inputs to outputs). In the context of rule extraction from data, FL as well models only continuous types, *at least initially*. After an initial FIS is formed, particular MFs can be modified so as to make the input have rule firings only at discrete settings. Surely, this is a suboptimal approach, but any

capability is better than none. Of course, the accuracy of the FIS before and after such a modification should always be examined.

Overall, as is usually the case when comparing competing algorithms, neither FL nor RSM is the better choice all of the time. However, through examination of concept fundamentals as well as examples, this initial investigation has identified the types of scenarios in which each would be best utilized.

5. Future Directions in Robust Design

Besides the work in progress described above, research in years two and three of this study will be initiated in the area of Fast Probability Integration (FPI). FPI encompasses a number of techniques which show promise in replacing the computationally intense Monte Carlo approach to generating probability distributions in the RDS setting. Many of these techniques have developed in the fields of reliability and structural failure/fatigue prediction. Fundamentally, however, they are appropriate for any situation where uncertainty is to be quantified and eventually mitigated to the largest extent possible. Studies in Reference 14 [Wu] have shown that FPI can require from 1/10 to 1/1000 of the computer time as compared to Monte Carlo.

Steps already taken to incorporate FPI into RDS consist of the following:

a) The attendance of Dr. Mavris at a short course hosted by the Southwest Research Institute entitled "Probabilistic Analysis and Design- Computational Methods and Applications". This short course provided a much needed survey of what FPI methods are currently being proposed/used in industry, government, and industry.

b) A visit of Dr. Mavris with Dr. Christos Chamis of NASA Lewis, who has developed several approaches and codes for probabilistic structural analysis and design. This visit resulted in an agreement between ASDL and Dr. Chamis' branch for the sharing of information and codes related to FPI and probabilistic modeling.

6. Conclusions and Status

This report has documented Year one progress in this effort to develop "Advanced Design Methodology for Robust Aircraft Sizing and Synthesis". This was done via a detailed development of the proper objective function in a robust design setting. This objective, which best captures the customer requirements, is the probability of achieving a specified target(s) for an aircraft system (such as required yield per revenue passenger mile, $/RPM). After the development and explanation of this objective, differing types of uncertainty which enter an aircraft synthesis problem were described and methods for addressing these different types were explained (and demonstrated via example). Keys to implementing these methods were the Response Surface Method (RSM) and the Monte Carlo approach to probability distribution generation. While these techniques proved effective, deficiencies were identified in their use.

In looking toward the future (with Year two goals in mind), new techniques were investigated under the Year one effort in the hopes of mitigating the identified deficiencies in RSM and Monte Carlo. Descriptions of Neural Networks and Fuzzy Logic and their potential use in a robust design environment were presented. Finally, the Fast Probability Integration (FPI) technique seems promising as a efficient replacement to the computationally intense Monte Carlo method.

7. References

1 Decisioneering, Inc., Crystal Ball Computer Program and User's Guide, Version 4.0, Aurora, CO, 1996.

2 Mavris, D.N., Bandte, O., and Brewer, J.T., *A Method for the Idenfication and Assessment of Critical Technologies Needed for an Economical Viable HSCT*, 1st AIAA Aircraft Engineering, Technology and Operations Congress, Los Angeles, CA, September , 1995, AIAA 95-3887.

3 Galloway, T.L., and Mavris, D.N., *Aircraft Life Cycle Cost Analysis (ALCCA) Program*, NASA Ames Research Center, September 1993.

4 Mavris, D.N., Bandte, O., "Application of Probabilistic Methods for the Determincation of an Economically Robust HSCT Configuration", AIAA/USA/NASA/ISSMO Multidisciplinary Analysis and Optimization Conference, Bellevue, WA, September 4-6, 1996.

5 DeLaurentis, D.A., Mavris, D.N., Schrage, D. P., "An IPPD Approach to the Preliminary Design Optimization of an HSCT using Design of Experiments", to be presented at 20th ICAS Congress, Sorrento, Italy, 8-13 September 1996.

6 SAS Institute Inc., <u>JMP Computer Program and User's Manual</u>, Cary, NC, 1994.

7 Ref. Roth

8 Sakata, I.F., and Davis, G.W., "Evaluation of Structural Design Concepts for Arrow-Wing Supersonic Cruise Aircraft," NASA CR-2667, May, 1977.

9 *MATLAB- Neural Network Toolbox User's Guide*, The Math Works, Inc., Natick, MS, January 1994 .

10 Seguno, M., "An Introductory Survey of Fuzzy Control", *Information Science*, Vol. 36, pp. 59-83, 1985.

11 Tong, R.M., "The Evaluation of Fuzzy Models Derived from Experimental Data", *Fuzzy Sets and Systems*, Vol. 4, pp. 1-12, 1980.

12 *MATLAB- Fuzzy Logic Toolbox User's Guide*, The Math Works, Inc., Natick, MS, January, 1995.

13 Chiu, S., "Extracting Fuzzy Rules from data for Function Approximation and Pattern Classification", Proc. *7th Annual Rockwell International Conference on Control and Signal Processing*, Thousand Oaks, CA, May 1995.

14 Wirsching, P.H., Wu, Y.T., <u>Transactions of ASME</u> Volume 109, February 1987.

Title: Advanced Design Methodology for Robust
Aircraft Sizing and Synthesis
Report: Performance Report
Period: January 22, 1997 - November 21, 1997

Submitted to:

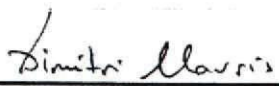**NASA Langley Research Center**
Mail Stop 126
Hampton, VA 23681-0001

Technical Contact: Dr. Gary L. Giles
Sponsor Contact: Ms. Marcia Poteat

NAG-1-1793

Submitted By:

Dr. Dimitri N. Mavris
AEROSPACE SYSTEMS DESIGN LABORATORY
SCHOOL OF AEROSPACE ENGINEERING
GEORGIA INSTITUTE OF TECHNOLOGY
A Unit of the University System of Georgia
Atlanta, GA 30332-0150

November 11, 1997

SUMMARY OF CONTRACT PERIOD EFFORTS

Contract efforts are focused on refining the Robust Design Methodology for Conceptual Aircraft Design. Robust Design Simulation (RDS) was developed earlier as a potential solution to the need to do rapid trade-offs while accounting for risk, conflict, and uncertainty. The core of the simulation revolved around Response Surface Equations as approximations of bounded design spaces.

An ongoing investigation is concerned with the advantages of using Neural Networks in conceptual design. In the overall design methodology, one possibility for the application of Neural Networks is as an alternative to the Response Surface Equations, which are limited in both the number of parameters and their ranges. To investigate this, a first step was to implement a two-layer (one hidden layer) feed-forward neural network with pure linear and tangent sigmoidal transfer functions to approximate the design metrics of various disciplines and bring them back to the systems level. Some aspects in this approach were found to need special attention. Among them are the selection of the number of neurons in the hidden layer, which were adjusted with the learning behavior, and the appropriate training methods for the neural network. The network was trained via backpropagation methods, and the development of suitable training methods will lead to genetic algorithms and other methods to be used for this purpose.

Thought was also given to the development of a systematic way to choose or create a baseline configuration based on specific mission requirements. To explore the possibilities of Knowledge-Based Systems with their reasoning and database mining capabilities, an Expert System was developed, which selects aerodynamics, performance and weights models from several configurations based on the user's mission requirements for subsonic civil transports. This motivates future research toward investigating a hybrid system of artificial intelligence methods, possibly Neural Networks combined with Knowledge-Based Systems, to systematically select or develop baseline configurations for unconventional aircraft designs. In addition, such a hybrid system can potentially provide design guidance in the larger scope of the overall RDS.

The investigation of affordability in the design process has made the investigation of a probabilistic approach to design necessary, due to the inherent ambiguity of assumptions and requirements as well as the uncertain operating environment of future aircraft. The approach previously developed at ASDL, linking Response Surface Methodology with Monte Carlo Simulations, has revealed itself to be cumbersome and at times impractical for multi-constraint, multi-objective problems. In addition, prediction accuracy problems were observed for certain scenarios that could not easily be

resolved. Hence, a portion of this year's research focused on an alternate approach to probabilistic design, which is based on a Fast Probability Integration (FPI) technique. Critical reviews of the combined Response Surface Equation/ Monte Carlo Simulation methodology against the Advanced Mean Value (AMV) method, one of several FPI techniques, has been accomplished. Both methods are used to generate cumulative distribution functions, which are subsequently compared in an example case studies, usually employing a High Speed Civil Transport (HSCT) concept. Outcomes of this research and the case studies have been an assessment and comparison of the analysis effort and time necessary for both methods is performed. In summarizing the results, the Advanced Mean Value method shows significant time savings over the Response Surface Equation/Monte Carlo Simulation method, and generally yields more accurate CDF distributions. The research has also resulted in a step-by-step illustration on how to use the AMV method for distribution generation and the search for robust design solutions to multivariate constrained problems.

Title: Advanced Design Methodology for Robust
Aircraft Sizing and Synthesis
Report: Performance Report
Period: January 22, 1997 - November 21, 1997

Submitted to:

NASA Langley Research Center
Mail Stop 126
Hampton, VA 23681-0001

Technical Contact: Dr. Gary L. Giles
Sponsor Contact: Ms. Marcia Poteat

NAG-1-1793

Submitted By:

Dr. Dimitri N. Mavris
AEROSPACE SYSTEMS DESIGN LABORATORY
SCHOOL OF AEROSPACE ENGINEERING
GEORGIA INSTITUTE OF TECHNOLOGY
A Unit of the University System of Georgia
Atlanta, GA 30332-0150

November 11, 1997

SUMMARY OF CONTRACT PERIOD EFFORTS

Contract efforts are focused on refining the Robust Design Methodology for Conceptual Aircraft Design. Robust Design Simulation (RDS) was developed earlier as a potential solution to the need to do rapid trade-offs while accounting for risk, conflict, and uncertainty. The core of the simulation revolved around Response Surface Equations as approximations of bounded design spaces.

An ongoing investigation is concerned with the advantages of using Neural Networks in conceptual design. In the overall design methodology, one possibility for the application of Neural Networks is as an alternative to the Response Surface Equations, which are limited in both the number of parameters and their ranges. To investigate this, a first step was to implement a two-layer (one hidden layer) feed-forward neural network with pure linear and tangent sigmoidal transfer functions to approximate the design metrics of various disciplines and bring them back to the systems level. Some aspects in this approach were found to need special attention. Among them are the selection of the number of neurons in the hidden layer, which were adjusted with the learning behavior, and the appropriate training methods for the neural network. The network was trained via backpropagation methods, and the development of suitable training methods will lead to genetic algorithms and other methods to be used for this purpose.

Thought was also given to the development of a systematic way to choose or create a baseline configuration based on specific mission requirements. To explore the possibilities of Knowledge-Based Systems with their reasoning and database mining capabilities, an Expert System was developed, which selects aerodynamics, performance and weights models from several configurations based on the user's mission requirements for subsonic civil transports. This motivates future research toward investigating a hybrid system of artificial intelligence methods, possibly Neural Networks combined with Knowledge-Based Systems, to systematically select or develop baseline configurations for unconventional aircraft designs. In addition, such a hybrid system can potentially provide design guidance in the larger scope of the overall RDS.

The investigation of affordability in the design process has made the investigation of a probabilistic approach to design necessary, due to the inherent ambiguity of assumptions and requirements as well as the uncertain operating environment of future aircraft. The approach previously developed at ASDL, linking Response Surface Methodology with Monte Carlo Simulations, has revealed itself to be cumbersome and at times impractical for multi-constraint, multi-objective problems. In addition, prediction accuracy problems were observed for certain scenarios that could not easily be

resolved. Hence, a portion of this year's research focused on an alternate approach to probabilistic design, which is based on a Fast Probability Integration (FPI) technique. Critical reviews of the combined Response Surface Equation/ Monte Carlo Simulation methodology against the Advanced Mean Value (AMV) method, one of several FPI techniques, has been accomplished. Both methods are used to generate cumulative distribution functions, which are subsequently compared in an example case studies, usually employing a High Speed Civil Transport (HSCT) concept. Outcomes of this research and the case studies have been an assessment and comparison of the analysis effort and time necessary for both methods is performed. In summarizing the results, the Advanced Mean Value method shows significant time savings over the Response Surface Equation/Monte Carlo Simulation method, and generally yields more accurate CDF distributions. The research has also resulted in a step-by-step illustration on how to use the AMV method for distribution generation and the search for robust design solutions to multivariate constrained problems.

Title: Advanced Design Methodology for Robust Aircraft
Sizing and Synthesis
Report: Performance Report
Period: 22-Jan-98 through 21-Nov-98

Submitted to:

NASA Langley Research Center
Mail Stop 126
Hampton, VA 23681-0001

Technical Contact: Mr. Paul Gelhausen
Sponsor Contact: Ms. Marcia Poteat

NAG-1-1793

Submitted by:

Dr. Dimitri N. Mavris
AEROSPACE SYSTEMS DESIGN LABORATORY
SCHOOL OF AEROSPACE ENGINEERING
GEORGIA INSTITUTE OF TECHNOLOGY
Atlanta, GA 30332-0150

November 17, 1998

SUMMARY OF ACCOMPLISHMENTS FOR CURRENT CONTRACT PERIOD

The goal of designing for robustness is achieved by minimizing a configuration's sensitivity to the uncertainty factors, which themselves may take various forms (economic, mission related, disciplinary). The result is a solution which satisfies the customer requirements while at the same time is well-balanced in that it performs well under a wide variation of conditions. Over the term of this grant, research has led to a series of methods by which robust aircraft designs are obtained utilizing a probabilistic objective function and techniques such as Response Surface Method and Monte Carlo simulation.

For the period covering this performance report, the advanced robust design method(s) has been refined, formalized, and expanded to include the evaluation of new technologies. The majority of this work has been summarized and disseminated in three conference papers published as well as one journal article accepted for publication in February, 1999. These documents are listed below and are available at: http://www.asdl.gatech.edu/publications

1. Mavris, D.N., DeLaurentis, D.A., "A Stochastic Design Approach for Aircraft Affordability," 21st Congress of the International Council on the Aeronautical Sciences (ICAS), Melbourne, Australia, September 1998. Paper ICAS-98-6.1.3.

2. Mavris, D.N., Kirby, M.R., Qiu, S., "Technology Impact Forecasting for a High Speed Civil Transport", World Aviation Congress and Exposition, Anaheim, CA, September 28-30, 1998. SAE-985547.

3. Daberkow, D.D., Mavris, D.N., "New Approaches to Conceptual and Preliminary Aircraft Design: A Comparative Assessment of a Neural Network Formulation and a Response Surface Methodology", World Aviation Congress and Exposition, Anaheim, CA, September 28-30, 1998. SAE-985509.

A major accomplishment in the first two years of this research was the construction of a probabilistic design method that identified when a new technology infusion would be required to increase the robustness of the design (e.g. its chances of success). In this last year, research has focused on how one goes about modeling and assessing the impact of these new technologies and the feasibility and viability of the design space. The response surface method is again used in what has become known as a Technology Impact Forecast (TIF) environment (see papers 1. and 2. referenced above). The variability due to uncertainty in technology performance can now be accounted for in forecasting future design performance. The TIF was implemented for the High Speed Civil Transport as reported in papers 1. and 2.

Several tools that aid in the exercising of these methods are shown in the following table. An asterisk indicates the specific tools that were given to the sponsor for their future use.

SOFTWARE	PURPOSE
STARS[*]	Utility to aid in the setup of Design of Experiments information and its execution
Command Line DOE[*]	Utility to aid in the setup of Design of Experiments tables from JMP
parse[*], tsw[*]	Automatable I/O file parsing and substitution utilities
plotcdf[*]	Plots Cumulative distribution function from FPI output
doe2rse[*]	Regression of DOE data for a specified model equation
JMP[o]	Commercial statistical analysis package by SAS Institute Inc.
Crystal Ball[o]	Commercial Monte Carlo Sim. package by Decisioneering Inc.

Finally, as an extension of earlier work on the use of the RSM, research into alternative approximation and optimization techniques has continued, primarily in the area of neural networks. Paper 3. referenced above has documented a study of the relative merits of RSM and neural networks in the robust design setting. A key conclusion from this investigation was that the networks can indeed outperform RSM, especially when the underlying nature of the problem is unknown and the number of necessary factors is high.

All the above activities were reported to the technical monitor directly in a visit on October 16/17, 1998 at Georgia Tech.

Title: Advanced Design Methodology for Robust Aircraft
Sizing and Synthesis
Report: Performance Report
Period: 22-Jan-98 through 21-Nov-98

Submitted to:

NASA Langley Research Center
Mail Stop 126
Hampton, VA 23681-0001

Technical Contact: Mr. Paul Gelhausen
Sponsor Contact: Ms. Marcia Poteat

NAG-1-1793

Submitted by:

Dr. Dimitri N. Mavris
AEROSPACE SYSTEMS DESIGN LABORATORY
SCHOOL OF AEROSPACE ENGINEERING
GEORGIA INSTITUTE OF TECHNOLOGY
Atlanta, GA 30332-0150

November 17, 1998

SUMMARY OF ACCOMPLISHMENTS FOR CURRENT CONTRACT PERIOD

The goal of designing for robustness is achieved by minimizing a configuration's sensitivity to the uncertainty factors, which themselves may take various forms (economic, mission related, disciplinary). The result is a solution which satisfies the customer requirements while at the same time is well-balanced in that it performs well under a wide variation of conditions. Over the term of this grant, research has led to a series of methods by which robust aircraft designs are obtained utilizing a probabilistic objective function and techniques such as Response Surface Method and Monte Carlo simulation.

For the period covering this performance report, the advanced robust design method(s) has been refined, formalized, and expanded to include the evaluation of new technologies. The majority of this work has been summarized and disseminated in three conference papers published as well as one journal article accepted for publication in February, 1999. These documents are listed below and are available at: http://www.asdl.gatech.edu/publications

1. Mavris, D.N., DeLaurentis, D.A., "A Stochastic Design Approach for Aircraft Affordability," 21st Congress of the International Council on the Aeronautical Sciences (ICAS), Melbourne, Australia, September 1998. Paper ICAS-98-6.1.3.

2. Mavris, D.N., Kirby, M.R., Qiu, S., "Technology Impact Forecasting for a High Speed Civil Transport", World Aviation Congress and Exposition, Anaheim, CA, September 28-30, 1998. SAE-985547.

3. Daberkow, D.D., Mavris, D.N., "New Approaches to Conceptual and Preliminary Aircraft Design: A Comparative Assessment of a Neural Network Formulation and a Response Surface Methodology", World Aviation Congress and Exposition, Anaheim, CA, September 28-30, 1998. SAE-985509.

A major accomplishment in the first two years of this research was the construction of a probabilistic design method that identified when a new technology infusion would be required to increase the robustness of the design (e.g. its chances of success). In this last year, research has focused on how one goes about modeling and assessing the impact of these new technologies and the feasibility and viability of the design space. The response surface method is again used in what has become known as a Technology Impact Forecast (TIF) environment (see papers 1. and 2. referenced above). The variability due to uncertainty in technology performance can now be accounted for in forecasting future design performance. The TIF was implemented for the High Speed Civil Transport as reported in papers 1. and 2.

Several tools that aid in the exercising of these methods are shown in the following table. An asterisk indicates the specific tools that were given to the sponsor for their future use.

SOFTWARE	PURPOSE
STARS[*]	Utility to aid in the setup of Design of Experiments information and its execution
Command Line DOE[*]	Utility to aid in the setup of Design of Experiments tables from JMP
parse[*], tsw[*]	Automatable I/O file parsing and substitution utilities
plotcdf[*]	Plots Cumulative distribution function from FPI output
doe2rse[*]	Regression of DOE data for a specified model equation
JMP[©]	Commercial statistical analysis package by SAS Institute Inc.
Crystal Ball[©]	Commercial Monte Carlo Sim. package by Decisioneering Inc.

Finally, as an extension of earlier work on the use of the RSM, research into alternative approximation and optimization techniques has continued, primarily in the area of neural networks. Paper 3. referenced above has documented a study of the relative merits of RSM and neural networks in the robust design setting. A key conclusion from this investigation was that the networks can indeed outperform RSM, especially when the underlying nature of the problem is unknown and the number of necessary factors is high.

All the above activities were reported to the technical monitor directly in a visit on October 16/17, 1998 at Georgia Tech.

Title: Advanced Design Methodology for Robust Aircraft
Sizing and Synthesis

Report: Summary of Research Report

Period: January 22, 1996 to April 30, 1999

Submitted to:

NASA Langley Research Center
Mail Stop 126
Hampton, VA 23681-0001

Technical Contact: Mr. Paul Gelhausen
Sponsor Contact: Ms. Marcia Poteat

NAG-1-1793

Submitted by:

Dr. Dimitri N. Mavris
AEROSPACE SYSTEMS DESIGN LABORATORY
SCHOOL OF AEROSPACE ENGINEERING
GEORGIA INSTITUTE OF TECHNOLOGY
Atlanta, GA 30332-0150

July 28, 1999

SUMMARY OF ACCOMPLISHMENTS

Robust design is accomplished by minimizing a design's sensitivity to uncertainty factors, which may be economic, mission, or disciplinary related. The goal of robust design is to seek a solution that satisfies all customer requirements and performs well under a wide range of conditions. During the term of this grant, robust design problems have been formulated and solved by utilizing a probabilistic objective function and techniques like Response Surface Method (RSM), Monte Carlo Simulation (MCS), and Fast Probability Integration (FPI). In solving the robust design problem, research has led to several advanced robust design methodologies, and they have been refined, formalized, and expanded to include the evaluation of new technologies. The work performed under this grant has been summarized and disseminated in four conference papers and one journal article (listed below). They are available for download at http://www.asdl.gatech.edu/publications.

1. Mavris, D.N., DeLaurentis, D.A., "A Stochastic Design Approach for Aircraft Affordability," 21st Congress of the International Council on the Aeronautical Sciences (ICAS), Melbourne, Australia, September 1998. Paper ICAS-98-6.1.3.

2. Mavris, D.N., Kirby, M.R., Qiu, S., "Technology Impact Forecasting for a High Speed Civil Transport", World Aviation Congress and Exposition, Anaheim, CA, September 28-30, 1998, SAE-985547.

3. Daberkow, D.D., Mavris, D.N., "New Approaches to Conceptual and Preliminary Aircraft Design: A Comparative Assessment of a Neural Network Formulation and a Response Surface Methodology", World Aviation Congress and Exposition, Anaheim, CA, September 28-30, 1998. SAE-985509.

4. Mavris, D.N., Bandte, O., DeLaurentis, D.A., "Determination of System Feasibility and Viability Employing a Joint Probabilistic Formulation", 37th Aerospace Sciences Meeting & Exhibit, Reno, NV, January 11-14, 1999. AIAA 99-0183

5. Mavris, D.N., Bandte, O., DeLaurentis, D.A., "Robust Design Simulation: A Probabilistic Approach to Multidisciplinary Design," Journal of Aircraft, Volume 36, No. 1, Pages 298 – 307.

In the first two years, the major accomplishment was the construction of a probabilistic design method that identified when new technology infusion is needed in order to increase the robustness of the design (e.g. its chances of success). In this last year, research has focused on

how one goes about modeling and assessing the impact of these new technologies and the feasibility and viability of the design space. The Response Surface Method is again used in what has become known as a Technology Impact Forecast (TIF) environment (see papers 1 and 2 referenced above). The variability due to uncertainty in technology performance can now be accounted for in forecasting future design performance. The TIF was implemented for the High Speed Civil Transport as reported in papers 1 and 2.

Also, in the last year of this grant, a natural progression of the robust design methodology to examine the variability due to uncertainty for several different criteria simultaneously was completed. The research funds provided under this grant was used as "seed money" to investigate a joint probability formulation to see how multiple decision criteria can be addressed while handling uncertain information probabilistically. The initial findings of this research for two dimensions are documented in paper 4 listed above. This research has shown much potential; therefore it was proposed to the Sponsor and accepted as the next phase of research for advanced probabilistic/stochastic design methods.

Several prototype tools that aid in the exercising of these methods (excluding joint probability formulation) are shown in the following table. An asterisk indicates the specific prototype tools that were given to the sponsor for their future use.

SOFTWARE	PURPOSE
STARS[*]	Utility to aid in the setup of Design of Experiments information and its execution
Command Line DOE[*]	Utility to aid in the setup of Design of Experiments tables from JMP
parse[*], tsw[*]	Automated I/O file parsing and substitution utilities
plotcdf[*]	Plots Cumulative distribution function from FPI output
doe2rse[*]	Regression of DOE data for a specified model equation
JMP[e]	Commercial statistical analysis package by SAS Institute Inc.
Crystal Ball[e]	Commercial Monte Carlo Simulation package by Decisioneering Inc.

Finally, as an extension of earlier work on the use of the RSM, research into alternative approximation and optimization techniques has continued, primarily in the area of neural networks. Paper 3 referenced above has documented a study of the relative merits of RSM and neural networks in the robust design setting. A key conclusion from this investigation was that the networks can indeed outperform RSM, especially when the underlying nature of the problem is unknown and the number of necessary factors is high.

The final research area conducted during the no-cost-extension period was the use of the Fast Probability Integration. This technique was developed by Southwest Research Institute under sponsorship from NASA Glenn Research Center. The general idea behind FPI is the estimation of the probabilistic modeler instead of the analysis code, as with using Response Surface Methodology. By eliminating the approximation of the physic-based codes, the probabilistic design methods, which is essential to robust design, is now much more practical and accurate.

All the above activities, excluding the joint probability formulation and FPI, were reported to the technical monitor directly in a visit on October 16 and 17, 1998 at Georgia Tech.